

Authors are grateful for constructive comments from all the referees that helped to improve the manuscript. A point-by-point response to the reviews and a list of all relevant changes can be found below. A marked-up manuscript version is added at the end of the document.

Response to RC1: 'Comments on tc-2019-148',

This is an extremely interesting paper and represents a large step forward in efforts to understand the distribution of permafrost temperature in the Antarctic. It is a novel contribution and will likely be a benchmark set of predictions for years to come.

Comment: Much of the model work here relies on use of ERA-Interim reanalysis products and down-scaling. How do the reanalysis surface temperatures and precipitation values compare to measured surface temperatures and precipitation values at long-term monitoring sites? The model will only be as good as the measurements that underlie it, and microclimate conditions dominate many ice-free areas.

Response: The ERA reanalysis near-surface temperature data dominates over MODIS LST only in very cloudy area as the Western Antarctic Peninsula. The ERA reanalysis quality significantly affects results in these regions, whereas it has less influence in areas with little cloud cover. Jones and Lister (2015) compared near surface temperatures between meteorological stations and ERA-Interim reanalysis and reported that bias for the stations outside the ice sheet is $-0.9\text{ }^{\circ}\text{C}$ with a RMSE of $1.96\text{ }^{\circ}\text{C}$, which is within the range of our model uncertainties. On the other hand, it is challenging to measure snowfall in the Antarctic, thus it is also difficult to estimate the accuracy of the snowfall used for the modelling.

Comment: One potential shortcoming of the model is that all surfaces are treated as having the same composition in terms of thermal properties. Yet IFAs can be either solid bedrock (with a variety of different lithologies possible), or soil, or ice cemented soil. How much of the overall uncertainty in the model can be attributed to the choice of subsurface thermal properties? What about active layer characteristics? Where present, wet active layers may significantly increase heat transport into the surface, while dry active layers serve to insulate permafrost.

Response: The authors would be very happy to include any information about ground properties for defining r_k -factor, but such information is available only for very limited areas in the Antarctic and no suitable product is available for pan-Antarctic scale. The used TTOP model calculates only MAGTs without taking in to account any active layer properties. The only way that lithology influences the modelled results is through the r_k -factor, which is a ratio between thawed and frozen thermal conductivity. It is used to scale TDDs thus it has affect only on results where TDDs are considerably high. The majority of the Antarctic regions have very little or no TDDs, thus the effect of using wrong r_k -factors is negligible in most areas. A sensitivity test on the Antarctic Peninsula, where TDDs are the highest, showed that considerable changes in r_k -factors had relatively small differences in the resulting MAGTs, which were in order of a few $0.1\text{ }^{\circ}\text{C}$.

Changes: A paragraph discussing potential shortcomings regarding the thermal properties of the ground and r_k -factors was added to the section 4.3

Comment: There are abundant examples of unclear English usage in this paper that should be addressed by a copy editor prior to submission. Many are small, e.g., “the temperature” when “temperature” would suffice, but they are too numerous for me to highlight individually.

Response: The English language has been reviewed by a competent native English speaking technical writer and corrected as appropriate.

Specific Comments.

Comment: P1, Line 20. “under” seems like a slightly odd word choice. Technically, it is mostly correct, since in most ice-free areas there is an active layer, although, not all ice-free areas have active layer conditions. For that reason, “within” might be a more accurate word to use here and throughout, unless subsurface temperatures are being discussed. See, P2, L2

Changes: Changed accordingly to within

Comment:: P1, Line 21. “a” is not needed here

Changes: Changed accordingly

Comment: P2, L2-4. This sentence has several unclear uses of language and should be revised.

Response: The second part of the sentence was removed.

Changes: Sentence shortened to: “Permafrost in the Antarctic is present beneath all ice-free terrain, except for the lowest elevations of the maritime Antarctic and sub-Antarctic islands (Vieira et al., 2010).”

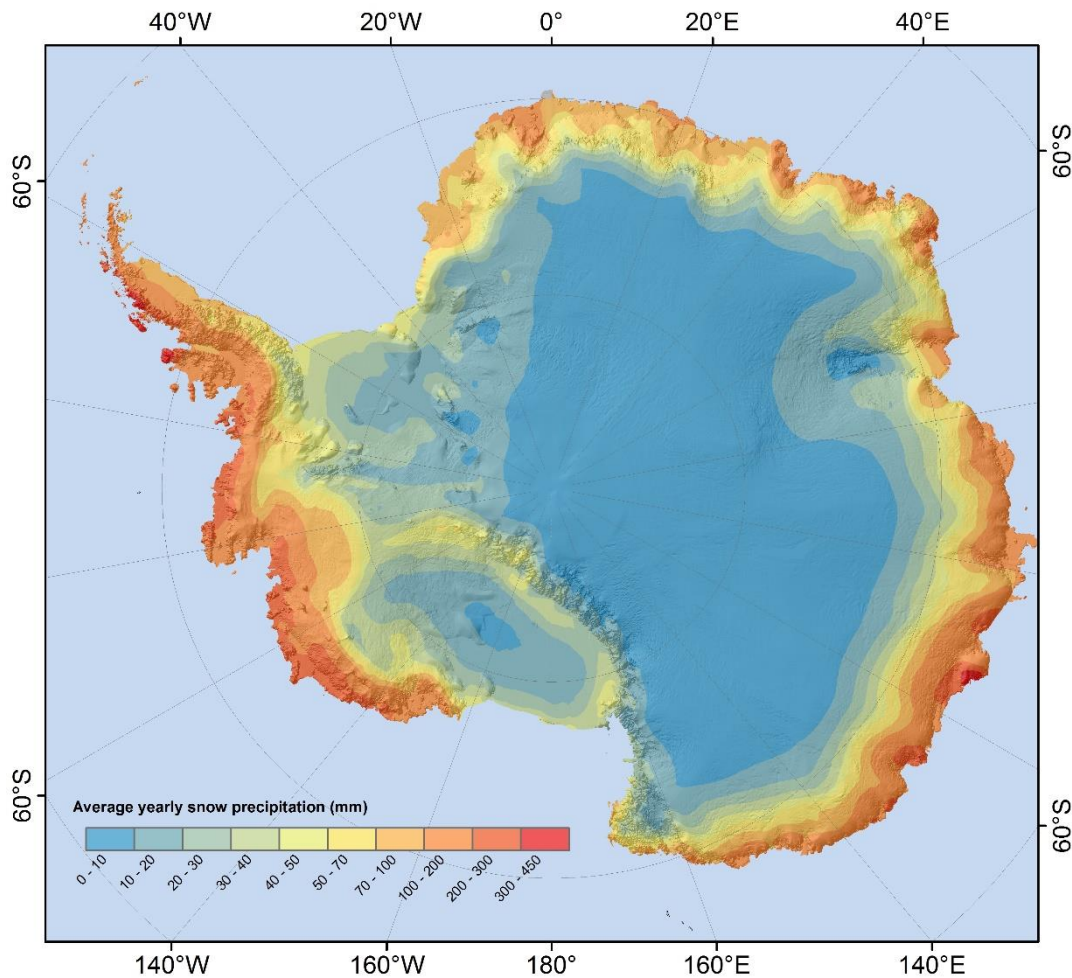
Comment: P2, L4. The Landsat-based reconstructions of ice-free area were conducted even earlier in the largest IFA by Levy (2012).

Response: We report only an ice-free area for the whole Antarctic in this part of the paper. The calculations from Burton-Johnson et al. (2016) were corrected by Hrbáček et al. (2018) and this is the reason that the both studies are cited.

Changes: The area was updated for McMurdo Dry Valleys in the section 3.6.1

Comment: P5, L14. There is commonly not just an elevation gradient in Antarctica, but also a coastal-inland gradient for precipitation. How does proximity to coastal moisture sources affect snow cover at inland sites?

Response: The snowfall was downscaled from Era-Interim and ERA-5 to 1 km² spatial resolution. The coastal-inland gradients seem to be well represented as shown on the figure below.



Comment: P6, L10. rk of 0.85 seems very high—especially for sandy, low-organic permafrost typical of the Transantarctics. (McKay et al., 1998) report thermal conductivities of thawed and ice-cemented permafrost of 0.6 and 2.5 W/mK, respectively, which would be less than 1/3 of the proposed value. (Levy and Schmidt, 2016) report a range of wetted soil thermal conductivity values for similar cold desert soils, ranging from ~0.2 to ~1.7 W/mK, which are still on the low end compared to the frozen value. What is the impact of having such a high rk value?

Response: According to the input data, there are no thawing degree days in the Transantarctic region. TDDs at coastal sites contribute at most 0.2 % to the sum of TDDs and FDDs. Since only TDDs are multiplied by rk-factors in the TTOP model, the effect of rk factors is negligible in the Transantarctic region.

Comment: Fig. 3. It is a little bit confusing having different legends on the two maps, which show both datasets. Can you put both legends on both maps?

Response: Putting both legends on both panels would be feasible for this figure. Repeating this for all of the figures with two or more panels would mean significant increase in size of the figures, which already represent a significant part of the paper. The authors would therefore prefer just to state in the caption that legends are valid for all of the panels in the figure.

Changes: A sentence “Legends, scale, and north arrow are valid for both panels” was added to all figures with panels.

Comment: P13, L4. East of 90°E would be a more clear way to phrase this.

Changes: Changed accordingly.

Comment: Figs 3 – 14. I’d suggest thinking more about the color ramp used to present this temperature data. Why was it selected? Because it is not a single gradient or ramp, it is difficult to tell what color is warmer or cooler than which other color without consulting the legend. It is not extremely intuitive. Either a single color intensity ramp, or a red-blue or green-blue color ramp might be more clear.

Response:

The temperature ramp was created to represent the MAGTs for the Northern Hemisphere modelling with 21 classes that could not be distinguished using continuous colour ramp with only one or two colours and so many different hues. The same ramp was used also to represent MAGTs for the Antarctic. The warmer-coloured stretching from yellow to red was used for positive temperatures. Except for the Figure 14, there are no positive MAGTs to be displayed, so only the cold temperature part of the ramp, stretching from green, blue, purple to grey, was used for the most of the figures.

We believe that the chosen colour scheme is a good compromise between putting as much information as possible on the map and the ability for a scientific-targeted public to be able to read it and grasp continuity of the data. The authors would also prefer to keep the colour ramps consistent between the Northern Hemisphere and this paper.

Comment: P24, L10. Is part of the apparent lapse rate behavior that you have observed a function of changing substrate? In low elevation areas, tills and other soils may dominate, while at high elevations, ice-free areas are largely bedrock. How might this affect the apparent MAGT lapse rate?

Response: The observed lapse behaviour is not a function of changing substrates since this information was unfortunately not included in the model. Due to the low TDDs the substrate properties taken into account by differences in the rk-factors would not have much influence on the modelled results, especially in the coldest parts of the Antarctic.

Comment: P24, L14. The increase in MAGT with elevation at some sites is extremely curious. What do you attribute it to? Is this explained in P30, L25? It might be worth highlighting this curious result sooner.

Response: It is difficult to attribute this lapse rate behaviour to any specific phenomenon. The ice-free areas of similar elevation are scattered around different areas inside regions, which have differing continentality and latitude characteristics. The differences are, in our opinion, more likely to cause the MAGT increase with elevation than the wide-spread temperature inversions. The effect of the temperature inversions, however, cannot be excluded.

Changes: The following sentence was added: “The MAGT increase with elevation could be explained by presence of rock outcrops with similar elevation in different latitudes or in different settings regarding continentality.”

Comment: P27, L4. Given the importance of orientation and insolation in controlling ground surface temperature in Antarctic ice free areas, would it be worth adding an orientation factor to the model? Something like fraction of north-facing surfaces in the grid cell? With datasets like REMA now available, it might significantly reduce the offsets in these numerous “microclimate” sites?

Response: The authors already considered including microclimate differences due to different terrain exposition in the model for the Northern Hemisphere. Although simple, the TTOP model is physically based and integration of MAGST relationships with terrain and slope aspect would require establishment of physical relationships. These physical relationships are in respect to the TTOP model not known thus we decided not to include this relationship. An additional challenge are the input MODIS data, which are acquired vertically, so the temperature signal from vertical slopes is not captured.

Comment: P31, L5. An RMSE of 1.9°C is really pretty good, but it could be a substantial uncertainty for warmer permafrost sites. How does uncertainty scale with absolute or mean average temperature? Are there particularly warm sites that have high uncertainty? How might the distribution of uncertainty affect our understanding of which permafrost is at risk of thaw?

Response: The TTOP model is an equilibrium model and does not take in to account latent heat released upon thawing of ice-rich permafrost or delayed freezing under cooling conditions. MAGTs at the warm permafrost sites on the Antarctic Peninsula have mostly been underestimated, but in most cases the difference is less than 2 °C. The greatest uncertainties occur on nunataks where the snow cover has been considerably overestimated.

According to the validation data the uncertainties are not the greatest at warm permafrost sites, although higher uncertainties can be expected on the ice-rich sites that are subject to rapid permafrost warming. A transient permafrost model would have to be used to predict which permafrost is at risk of thaw.

References:

Jones, P. D. and Lister, D. H.: Antarctic near-surface air temperatures compared with ERA-Interim values since 1979, *International Journal of Climatology*, 35(7), 1354–1366, doi:[10.1002/joc.4061](https://doi.org/10.1002/joc.4061), 2015.

Response to RC2: 'Review2'

Comment: 1. Since the model relies heavily on input data such as satellite observation, it is best to include uncertainty ranges for areas where satellite observations are lacking (cloudy days) or low quality. Otherwise it is wrong to advertise these model results as a generally accepted guideline for Antarctic permafrost conditions.

Response: The missing satellite data is gap-filled with ERA-Interim and ERA-5 reanalysis. The gap-filling method is based on several previous studies such as Westermann et al., (2015) and Obu et al (2019), where the improvement of the surface temperature data was discussed in detail. The greatest uncertainty is related to MODIS LST contamination by cloud temperatures. A percentage of MODIS

LST measurements in the gap-filled temperature dataset can be considered as a measure for the input satellite data.

Changes: The percentage of MODIS LST measurements in the combined MODIS/ERA surface temperature product are now included in Figure 1.

Comment: 2. Figures can be improved by proper color choice following other referee's suggestions. Also an overall figure of whole Antarctica with the modelled MAGT should be added at the end to give a general idea of MAGT in the whole continent to guide future studies. Forcing data uncertainty can be added to that figure.

Response: The authors had to make a compromise between how intuitive the colour ramps are and how much information can be put on the maps. Using intuitive colour ramps with one or two colours would make impossible to distinguish the number of the temperature classes that are presented on the maps. To be consistent between the studies, we prefer to keep the colour ramps the same as those that were used for the Northern Hemisphere by Obu et al. (2019). We also believe that the colour scheme is a good compromise between putting as much information as possible on the map and the ability for a scientific-targeted public to be able to read it and grasp continuity of the data.

The scale of the rock outcrops is so small in respect to the ice areas, that it is cartographically impossible to show a raster dataset at an Antarctic-wide scale. Thus, several maps had to be created at a regional scale.

Comment: 3. The model limitations should also include possible sources of uncertainty for n_f , n_t , and r_k values such as different thermal properties, soil hydrological conditions etc. Also it would be helpful to mention Cryogrid's difference to process-based models that are mainly used for northern hemisphere permafrost studies.

Response: The model limitations according to the n_f -factors were described in detail in section 4.3. We omitted n_t factors in the TTOP model since we use land surface temperature instead of air temperature. Discussion about ground properties and r_k -factors is extended.

Changes: A whole paragraph was added (fourth paragraph in the new version) in section 4.3 regarding the different soil thermal properties and r_k -factors. A transient permafrost model was mentioned at the end of this paragraph.

Minor comments

Comment: - fig2: correct the mismatch MAE written on figure (-0.17) and in text (0.06)

Changes: Changed accordingly to -0.17 in the text

Comment: - stay consistent with abbreviations, MAGTs vs MAGTS (p8116) –

Changes: Changed accordingly to MAGTs, which is now plural of MAGT.

Comment: p2417 correct “The lapse rates are is indicating: : :”

Changes: Changed accordingly to “The lapse rates indicate...”

Comment: - for section 4, please add corresponding figure numbers when discussing specific sites

Changes: Changed accordingly.

Comment: - conclusion at p31lines1-3, snow cover and redistribution effects should be added as an important factor as seen from the validations of this paper

Response: We agree that snow cover is an important factor governing local scale permafrost temperature distribution.

Changes: Following sentence was added: "Snow cover, and snow redistribution have strong influence local permafrost temperature variations in the Antarctic"

References:

Obu, J., Westermann, S., Bartsch, A., Berdnikov, N., Christiansen, H. H., Dashtseren, A., Delaloye, R., Elberling, B., Etzelmüller, B., Kholodov, A., Khomutov, A., Kääb, A., Leibman, M. O., Lewkowicz, A. G., Panda, S. K., Romanovsky, V., Way, R. G., Westergaard-Nielsen, A., Wu, T., Yamkhin, J. and Zou, D.: Northern Hemisphere permafrost map based on TTOP modelling for 2000–2016 at 1 km² scale, *Earth-Science Reviews*, 193, 299–316, doi:[10.1016/j.earscirev.2019.04.023](https://doi.org/10.1016/j.earscirev.2019.04.023), 2019.

Response to SC1: 'General comments',

Comment: 1. The mean absolute error in text is 0.06 C while on Fig.2 it is -0.017C.

Response: Corrected accordingly to -0.17 °C in the text.

Comment: 2. It is unclear what do authors mean by "values were set to randomly vary by 0.1 between 0.75 and 0.95" in section 2.5 with regards to rf parameter. Are values drawn from a uniform distribution between 0.75 and 0.95? What is the rationale behind the distribution of rf?

Response: The rk-factor values were drawn from a uniform distribution. The rationale is to simulate different ground properties in relation to soil moisture. Similar principles were used by Obu et al. (2019), where ranges of the rk-factors were defined by landcover classes. No similar information about ground properties was available for the Antarctic so the rk-factors from the literature were used to define limits.

Changes: The sentence was changed to: "Rk-factor values were drawn randomly from a uniform distribution to vary by ± 0.1 between 0.75 and 0.95."

Comment: 3. In section 2.2, it is unclear if the downscaled ERA-interim and ERA-5 near-surface temperatures were debiased towards MODIS record to create a consistent record. Since authors mention negative bias caused by data gaps wouldn't filling these gaps with near-surface temperature (which is not equivalent to surface temperature in general) provide additional bias to the record?

Response: The same procedure was used for this study as for the Obu et al. (2019). The gaps in MODIS data occur only during cloudy conditions when ground surface temperatures and air

temperatures are similar. The mentioned negative bias occurs due to having only clear-sky conditions in the MODIS record. Gap filling with ERA-interim and ERA-5 near-surface temperatures reduces this bias efficiently as demonstrated earlier by Westermann et al. (2015).

Comment: 4. In the same section (2.2), it is unclear why LST data was averaged to 8 day periods? Since FDD and TDD are essentially numerical integrals it is unclear why 8-day binning would give any advantage.

Response: The 8-day averages have been, in the first place, chosen to coincide with the period selected for MODIS longer-term averages (which are not bias-corrected). The gap-filling was applied to the 8-day periods, and the FDDs and TDDs were calculated from the same periods. The period of 8 days should be long enough, so that the applied gap-filling procedure becomes meaningful, i.e. there should be, at least on average, a few MODIS values, and the period is short enough that the yearly cycle can be reproduced, so that FDD and TDD can be meaningfully computed. We agree with the reviewer that one probably could have skipped the intermediate step by merging the gap-filling and FDDs and TDDs calculation, but we selected this method for consistency with Obu et al. (2019).

References:

Obu, J., Westermann, S., Bartsch, A., Berdnikov, N., Christiansen, H. H., Dashtseren, A., Delaloye, R., Elberling, B., Etzelmüller, B., Kholodov, A., Khomutov, A., Käab, A., Leibman, M. O., Lewkowicz, A. G., Panda, S. K., Romanovsky, V., Way, R. G., Westergaard-Nielsen, A., Wu, T., Yamkhin, J. and Zou, D.: Northern Hemisphere permafrost map based on TTOP modelling for 2000–2016 at 1 km² scale, *Earth-Science Reviews*, 193, 299–316, doi:[10.1016/j.earscirev.2019.04.023](https://doi.org/10.1016/j.earscirev.2019.04.023), 2019.

Westermann, S., Østby, T. I., Gislås, K., Schuler, T. V. and Etzelmüller, B.: A ground temperature map of the North Atlantic permafrost region based on remote sensing and reanalysis data, *The Cryosphere*, 9(3), 1303–1319, doi:<https://doi.org/10.5194/tc-9-1303-2015>, 2015.

Additional changes:

Minimum modelled temperature was changed from -33 to -36 °C in the abstract and conclusion. The lower value is more likely to be a true modelled minimum because it corresponds with the ensemble member with the thinnest snow cover. Such conditions are more likely to prevail on the mountain tops which often have thin snow cover due to stronger wind than the conditions assumed in the ensemble mean of MAGTs.

Added reference for a background topography to Fig. 1: “Background topography on this and all following maps is from the Quantarctica 3 database (Roth et al., 2017).”

A number of small changes that did not influence scientific content of the paper but improved clarity and language are marked in the track change document.

Manuscript with marked-up changes:

Pan-Antarctic map of near-surface permafrost temperatures at 1 km² scale

Jaroslav Obu¹, Sebastian Westermann¹, Gonçalo Vieira², Andrey Abramov³, Megan Balks⁴, Annett Bartsch^{5,6}, Filip Hrbáček⁷, Andreas Käab¹, Miguel Ramos⁸

¹Department of Geosciences, University of Oslo, Oslo, Sem Sælands vei 1, 0371 Oslo, Norway

²Centre of Geographical Studies, Institute of Geography and Spatial Planning, University of Lisbon, R. Branca Edmée Marques, 1600-276 Lisbon, Portugal

³Institute of Physicochemical and Biological Problems in Soil Science, Russian Academy of Sciences, Pushchino, Russia

⁴Department of Earth and Ocean Sciences, University of Waikato, Hamilton, Private Bag 3105, New Zealand

⁵Zentralanstalt für Meteorologie und Geodynamik, Hohe Warte 39, Vienna, Austria

⁶now at b.geos GmbH, Vienna, Industriestrasse 1 2100 Korneuburg, Austria

⁷Department of Geography, Masaryk University, Kotlářská 2 61137 Brno, Czech Republic

⁸Department of Physics and Mathematics, University of Alcalá, Madrid, Campus universitario 28805 Alcalá de Henares, Spain

Correspondence to: Jaroslav Obu (jaroslav.obu@geo.uio.no)

Abstract

Permafrost is present ~~under~~within almost all of the Antarctic's ice-free areas but little is known about spatial variations of permafrost temperatures ~~outside~~except for a few areas with established ground temperature measurements. We modelled a temperature at the top of the permafrost (TTOP) for all the ice-free areas of ~~the~~ Antarctic mainland and Antarctic Islands at 1 km² resolution during 2000–2017. The model was driven by remotely-sensed land surface temperatures and down-scaled ERA-Interim climate reanalysis data and subgrid permafrost variability was simulated by variable snow cover. The results were validated against in-situ measured ground temperatures from 40 permafrost boreholes and the resulting root mean square error was 1.9 °C. The lowest near-surface permafrost temperature of ~~-3336~~ °C was modelled at Mount Markham in ~~the~~ Queen Elizabeth Range in the Transantarctic Mountains. This is the lowest permafrost temperature on Earth according to ~~the~~global scale modelling results ~~on global scale~~. The temperatures were most commonly modelled between -23 and -18 °C for mountainous areas rising above the Antarctic Ice Sheet and between -14 and -8 °C for coastal areas. The model performance was good where snow conditions were modelled realistically but errors of up to 4 °C ~~can occur~~occurred at sites with strong wind-driven redistribution of snow.

1 Introduction

Permafrost in the Antarctic is present beneath all ice-free terrain, except for the lowest elevations of the maritime Antarctic and sub-Antarctic islands (Vieira et al., 2010), ~~unlike the northern hemisphere, where permafrost underlies approximately 15 % of the unglaciated land. The ice~~. Ice- and snow-free land occupies 0.22% (30 900 km²) of ~~the whole Antarctic~~Antarctica (Burton-Johnson et al., 2016; Hrbáček et al., 2018). ~~The major~~Major ice-free areas include ~~the~~ Queen Maud Land, Enderby Land, the Vestfold Hills, Wilkes Land, the Transantarctic

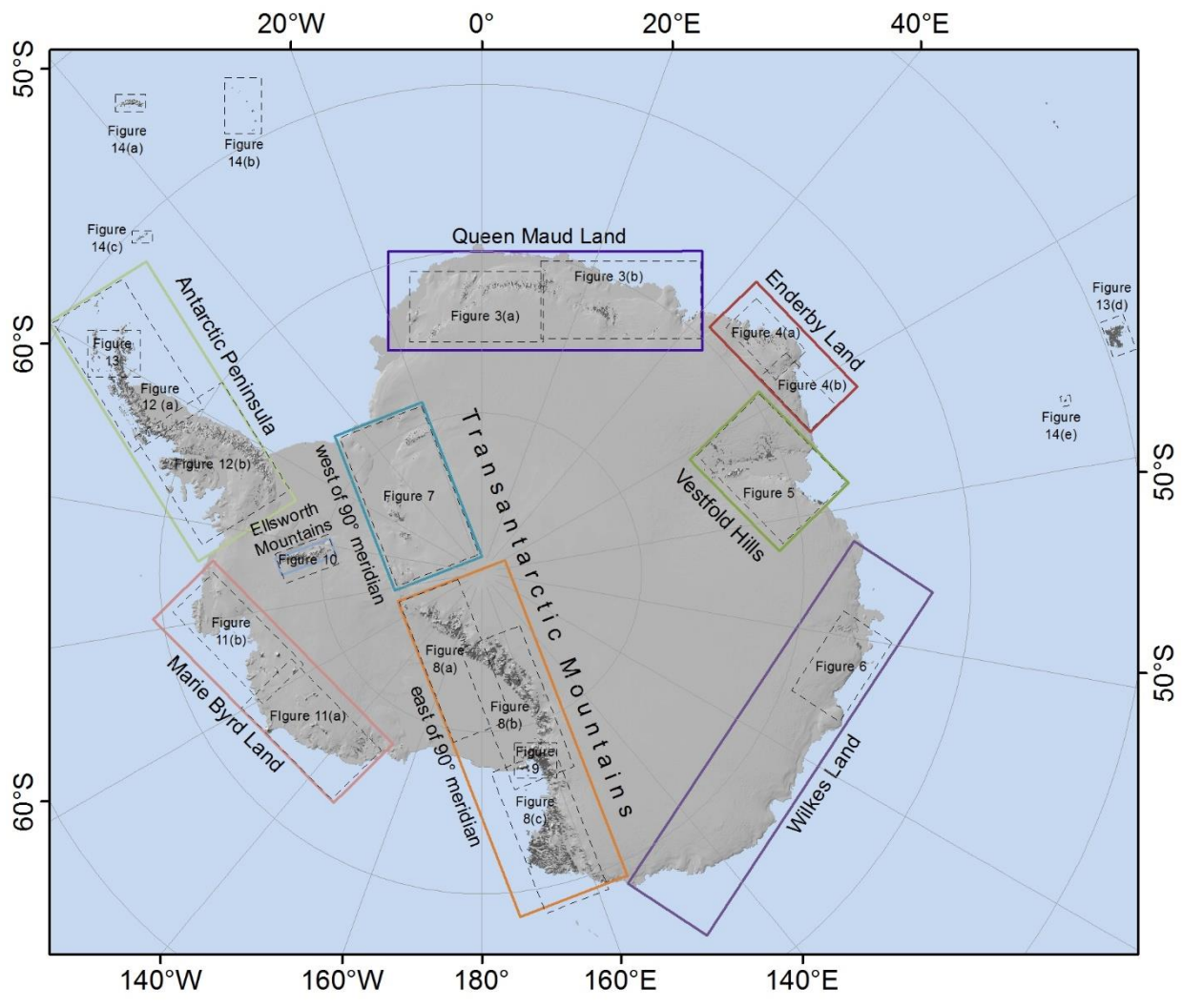
Mountains, the Ellsworth Mountains, Marie Byrd Land and the Antarctic Peninsula (Green et al., 1967; Fig. 1). Despite the relatively small area, in comparison to glaciated areas, permafrost is one of the major factors controlling terrestrial ecosystem dynamics in the Antarctic (Bockheim et al., 2008).

Compared with the Northern Hemisphere, where the first permafrost investigations date back to 19th century (Shiklomanov, 2005; Humlum et al., 2016), the ground temperatures in the Antarctic have been systematically studied only during the last two decades. Permafrost was studied in relation to patterned ground since the 1960s and during the Dry Valley Drilling Project in the 1970s but temperatures have been measured only occasionally (Decker and Bucher, 1977; Guglielmin, ~~2012~~2012a). A first Antarctic permafrost borehole network was implemented in 1999 in ~~the~~ Victoria Land (Transantarctic Mountains) and was extended during the International Polar Year 2007–2009 to cover all eight major ice-free regions (Vieira, 2010).

Permafrost distribution was estimated and mapped on the Antarctic Peninsula by Bockheim et al. (2013) based on mean annual temperature, periglacial features, shallow excavations, borehole measurements, geophysical surveys, and existing permafrost models. Bockheim et al. (2007) characterised permafrost in the McMurdo Dry Valleys based on ground ice properties and active layer thickness from more than 800 shallow excavations.

Antarctic permafrost modelling efforts were limited to small areas in the Antarctic Peninsula region and sub-Antarctic Islands. Ferreira et al. (2017) ~~used~~modelled freezing indexes and the temperature at the top of the permafrost (using TTOP) ~~modelling~~ for eight monitored sites on Hurd Peninsula ~~and~~ Livingston Island for the 2007 and 2009 seasons to study the controlling factors of ground temperatures. Rocha et al., (2010) ran the H-TESSEL scheme forced by ERA-Interim reanalysis to simulate ground temperatures at Reina Sofia Peak on Livingston Island. Ground temperature measurements and permafrost modelling efforts have been limited to point sites and little is known about spatial variability of ground temperatures at the regional and continent-wide scales.

In this study we employed the TTOP modelling scheme based on The Moderate Resolution Imaging Spectroradiometers (MODIS) land surface temperatures (LST) and ERA-Interim reanalysis to model the spatial distribution of temperatures at the top of permafrost on all ice-free areas of ~~Antaretic~~Antarctica and the Antarctic Islands. We ~~adapt~~adapted the existing modelling scheme from the Northern Hemisphere (Westermann et al., 2015; Obu et al., ~~2019~~2019a) according to the available input data and their characteristics for the Antarctic.



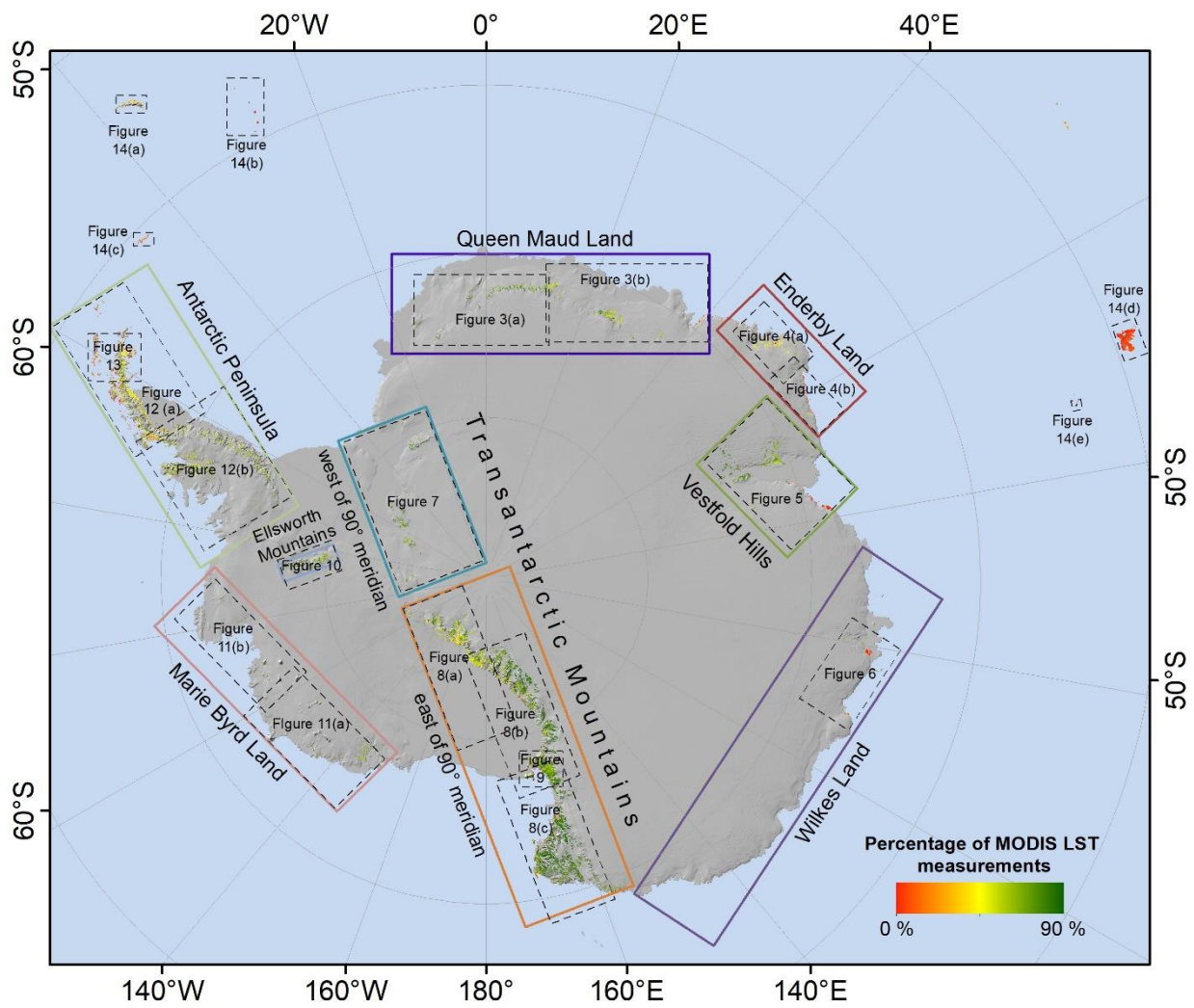


Figure 1: Overview map of the ice-free Antarctic regions and extents of the maps presented in the paper. The ice-free areas are shown according to percentage of MODIS LST measurements in the combined MODIS/ERA surface temperature product. Background topography, on this and all following maps, is from the Quantarctica 3 database (Roth et al., 2017).

2 Methods

2.1 The Cryogrid 1 model

The CryoGrid 1 model (Gisnås et al., 2013) calculates the mean annual ground temperature (MAGT) and is based on the TTOP equilibrium approach (Smith and Riseborough, 1996):

$$MAGT = \begin{cases} \frac{1}{\tau} (n_f FDD + r_k n_t TDD) \\ \text{for } (n_f FDD + r_k n_t TDD) \leq 0 \\ \frac{1}{\tau} (\frac{1}{r_k} n_f FDD + n_t TDD) \\ \text{for } (n_f FDD + r_k n_t TDD) > 0 \end{cases}$$

Where: FDD ~~and TDD represent~~ represents freezing ~~and degree days and TDD represents~~ thawing degree days, respectively, of in the surface meteorological forcing accumulated over the model period τ (in days-). The influence of ~~the~~ seasonal snow cover, vegetation, and ground thermal properties, were taken into account by the semi-empirical adjustment factors r_k (ratio of thermal conductivity of the active layer in thawed and frozen state), n_f (scaling factor between average winter surface and ground surface temperature) and n_t (scaling factor between average summer surface and ground surface temperature). We use land surface temperature (LST) to compute FDD and TDD (see following section) instead of the air temperature that was used initially by Smith and Riseborough (2002) and hence omit ~~the~~ thawing n_t -factors.

2.2 Freezing and thawing degree days

Spatially distributed data sets of TDD and FDD were compiled from remotely sensed land surface temperature products and climate reanalysis data following the procedure of Obu et al. (~~2019~~2019a). We used LST data (level 3 product in processing version 6) from MODIS on board the Terra and Aqua satellites, which contain up to two daytime and two night-time measurements per day at a spatial resolution of 1 km since the year 2000 (Wan, 2014). For this reason, the study extends from 2000 and to the end of 2017. Data gaps in the MODIS LST time series due to cloud cover can result in a systematic cold bias in seasonal averages (Westerman et al., 2012; Soliman et al., 2012; Østby et al., 2014), so a gap filling with near-surface air temperatures from the ERA-interim and ERA-5 reanalysis was applied (Westermann et al., 2015).

The ERA-interim reanalysis provides gap-free meteorological data from 1979 onwards at a spatial resolution of $0.75^\circ \times 0.75^\circ$ (Dee et al., 2011). The ERA-5 reanalysis is ERA-Interim upgrade and provides the data at improved $0.28125^\circ \times 0.28125^\circ$ (31 km) spatial resolution but was at the time of the study available only from 2008 onwards (Hersbach and Dee, 2016). ERA-Interim data were for this reason used before 2008 and ERA-5 data afterwards. The reanalysis data were downscaled to the 1 km resolution of individual MODIS pixels using atmospheric lapse rates and The Global Multi-resolution Terrain Elevation Data 2010 (GMTED2010) (Danielson and Gesch, 2011). The downscaling methodology ~~is was~~ described in detail by Fiddes and Gruber (2014), Westermann et al. (2015) and Obu et al. (~~2019~~2019a). The gap-filled MODIS LST time series were averaged to eight-day periods from which FDD and TDD were finally accumulated for the 2000–2017 study period.

2.3 Average annual snowfall and n_f -factors

Spatially distributed data sets of n_f -factors were generated from average annual snowfall forced by ERA-Interim and ERA-5 ~~reanalysis~~ reanalysed data. Snow cover in the majority of the Antarctic is dominated by sublimation

and processes related to blowing snow (Gallée, 1998; Bintanja and Reijmer, 2001), which were not taken in to account by the snowfall and degree-day model that Obu et al. (2019) used to estimate the n_f -factor for the Northern Hemisphere. ~~For this reason~~ Thus, only mean annual snowfall was calculated using the downscaled ERA-Interim precipitation data from before 2008 and the ERA-5 precipitation after 2008. Precipitation was downscaled based on the difference between reanalysis elevation data and GMTED2010 data using a precipitation gradient, found in drier areas (Hevesi et al., 1992), of 2 % per 100 m up to 1000 m and 1% per 100 m for elevations above 1000 m. Snowfall was defined as precipitation at air temperatures below 0 °C, using the downscaled ERA-Interim air temperatures as employed for the gap filling of MODIS LST (see above). For a detailed downscaling procedure description see Obu et al. (2019).

N_f -factors were defined based on average annual snowfall, however the reported n_f -factors in ~~Antaretic~~Antarctica were calculated in respect to snow depth. Oliva et al. (2017) identified n_f -factor values of around 0.3 for snow accumulations of 80 cm on Livingston Island, although the n_f -factors can reach up to 0.55 in the ~~thick snow covers~~ same accumulations due to ~~its~~their temporal variability (de Pablo et al., 2017). N_f -factors close to, or even greater than, one were measured in areas with little or no snow cover on Veleskarvet nunatak (Kotzé and Meiklejohn, 2017), in the McMurdo Dry Valleys (Lacelle et al., 2016) and on James Ross Island (Hrbáček et al., 2016). This range was used to constrain the n_f -factor ranges in relation to average annual snowfall (Table 1). Since the snow model was not able to simulate snow-free sites, nor snowdrifts, due to strong wind distribution, we used a maximum n_f -factor of 0.95 and a minimum of 0.3. However, smaller snow-depth variations on a local scale were taken into account with an ensemble of different values of average mean annual snowfall for each 1 km² pixel (e.g. Gislås et al., 2014).

Mean annual snowfall (mm)	n_f min	n_f max
< 3	0.85	0.95
3-10	0.77	0.85
10-30	0.75	0.77
30-50	0.73	0.75
50-75	0.67	0.73
75-100	0.64	0.67
100-125	0.55	0.64
125-150	0.5	0.55
150-200	0.45	0.5
200-300	0.4	0.45
> 300	0.3	0.4

Table 1: ranges of n_f -factors that were assigned to mean annual snowfall values.

2.4 r_k -factors

The r_k -factor is defined as the ratio of thawed and frozen thermal conductivities of the active layer material (Romanovsky and Osterkamp, 1995) and is related to water and organic matter contents (e.g. Gislén et al., 2013). Soil moisture properties were mapped on a regional scale (Bockheim et al., 2007) but no pan-Antarctic datasets related to soil water or organic contents were available. The ESA CCI Landcover that Obu et al. (2019, 2019a) used for the Northern Hemisphere study contains only a “permanent snow and ice” class on the Antarctic mainland, therefore, a rock outcrops dataset (Burton-Johnson et al., 2016) was used to constrain non-glaciated areas. An r_k -factor of 0.85 was used for the whole of the Antarctic, representing an average value between very dry sites on continental Antarctica and moderately moist sites on the Antarctic Peninsula.

2.5 Ensemble-based modelling of subpixel heterogeneity

Ground temperatures can vary considerably at short distances due to heterogeneous snow cover, vegetation, topography and soil properties (Beer, 2016; Gislén et al., 2014; 2016; Zhang et al., 2014). We ran an ensemble of 200 model realisations with different combinations of n_f - and r_k -factors to simulate the variability. r_k -factor values were ~~set to~~ randomly from a uniform distribution to vary by ± 0.1 between 0.75 and 0.95 to represent both very dry sites and locations with higher soil moisture. The distribution of snowfall within the 1 km pixel was simulated using a log-normal distribution function where mean annual snowfall determined the mean of the distribution. The coefficient of variation of the distribution for the open areas (0.9) according to Liston (2004) was assigned to all modelled areas. An n_f -factor was assigned to the estimated average annual snowfall according to Table 1. The pixels not overlapping with rock outcrops were masked out. A fraction of the model runs, with $MAGT < 0$ °C, was used to derive the permafrost type (zones) on Antarctic Islands (see Obu et al. (2019, 2019a) for detailed description).

2.6 Model validation

We compared our results to available in-situ measurements in 40 permafrost boreholes and shallow boreholes at soil-climate stations. The ensemble mean of modelled MAGTs was compared to the borehole measurements to take the simulated spatial variability, provided by the ensemble spread, into account. The accuracy of the model was estimated, with root mean square error (RMSE) and mean absolute error, between the modelled and measured MAGT.

The validation data were provided by the authors for the McMurdo Dry Valleys, ice-free areas near Russian stations (Bunger Hills, Schirmacher Hills, Larsemann Hills, Thala Hills, King George Island and Hobs coast) and the Northern Antarctic Peninsula. Ground temperatures from these locations represent mean MAGT at the top of the permafrost and usually overlap well with the modelling period 2000–2017 (Appendix A). Validation data for Queen Maud Land (Troll Station, Flarjuven Bluff, Vesleskarvet) and the Baker Rocks site were obtained from Hrbáček et al., (2018) and MAGTs from Terra Nova Bay (Oasi New and Boulder Clay) were obtained from Vieira et al., (2010). MAGTs from Hope Bay, Mt. Dolence, Marble Point Borehole and Limnopolar Lake were obtained from Schaefer et al. (2017a), Schaefer et al. (2017b), Guglielmin et al. (2011) and de Pablo et al.

(2014), respectively. The borehole data from Signy Island and Rothera Point were extracted from Guglielmin et al., (2012, 2012b) and (2014). The data ~~found~~reported in publications were not necessarily calculated for the top of the permafrost and do not completely overlap with the modelling period and are, thus, less reliable than the author-supplied validation data. For instance, the data from Vieira et al. (2010) represents MAGT for the periods before 2010 usually lasting only few years (Table 2).

3 Results

3.1 Comparison to borehole measurements

Ground temperatures can vary significantly inside a 1 km² model pixel, which is, to a certain extent, represented by the TTOP model ensemble runs. Average MAGT derived from the ensemble runs was compared to the measured site ground temperatures, which might limit representativeness for sites with locally specific ground and snow properties. The comparison yielded a RMSE of 1.94 °C and a mean absolute error for all boreholes of ~~-~~0.0617 °C (Fig. 2). The small mean absolute error is partly achieved with fine adjustment of the n_f -factor class limits. For 50 % of the boreholes, the agreement between borehole temperatures and modelled MAGT was better than 1 °C, while it is better than 2 °C for 75%, and better than 3 °C for 85 % of the boreholes. Assuming a Gaussian distribution of standard deviation σ MAGT, 68% of borehole comparisons should fall within one σ MAGT, while 95% falls within two σ MAGT, and 99% should be within three σ MAGT. For the comparison with Antarctic boreholes, 18 (45 %) boreholes were contained within one, 29 (73 %) within two, and 31 (78 %) within three standard deviations from the mean, which is comparable to the results for the Northern Hemisphere (Obu et al., 2019, 2019a).

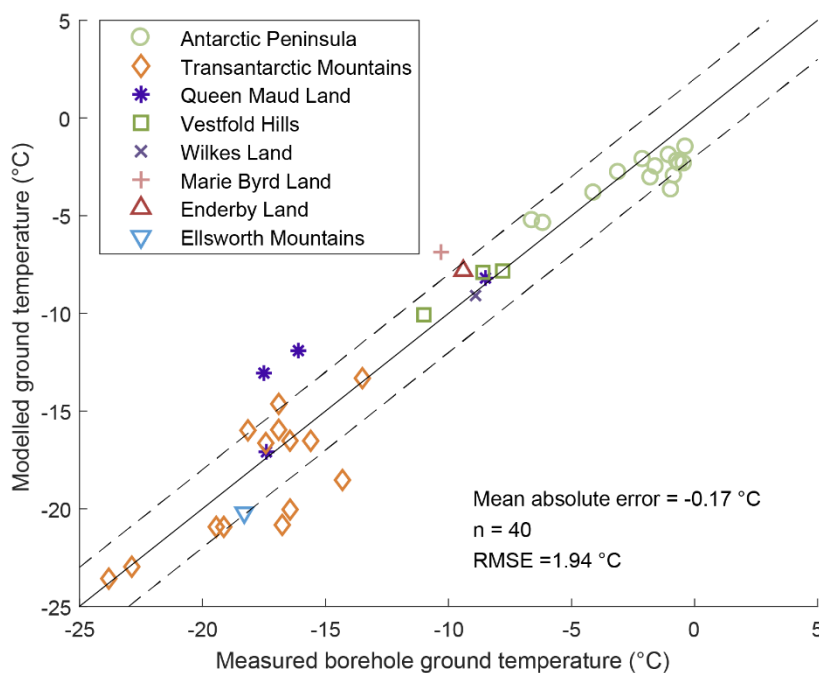


Figure 2: Measured vs. modelled permafrost temperatures for all boreholes. The dashed lines represent ± 2 °C intervals around the 1:1 solid line.

3.2 Queen Maud Land

There are ~~24302~~ 430 km² of ice free areas in Queen Maud Land according to the rock outcrop map (Burton-Johnson et al., 2016; Hrbáček et al., 2018). The average MAGT is -18.2 °C and it ranges from -26.2 °C in the highest parts of the Fimbulheimen Range to -6.3 °C ~~in~~on the Prince Olav Coast, where MAGTs down to -10 °C were modelled at elevations exceeding 200 m (Fig. 3). MAGTs above -10 °C can be found also at the Schirmacher Oasis (Hills) and reach above -8 °C. MAGTs in the Sør Rondane Mountains and in the Fimbulheimen Range range from -12 °C at elevations of around 800 m a.s.l. to -24 °C at elevations exceeding 3000 m a.s.l. The Kirwan Escarpment (elevations usually exceeding 2000 m) is characterised by ~~MAGTSMAGTs~~ between -23 °C and -20 °C and in the Heimefront Range (with slightly lower elevations) the MAGTs were between -22 °C and -18 °C. MAGTs ~~in Borg Massif were~~were modelled as being from -21 to -17 °C on the Borg Massif and between -16 and -12 °C ~~in~~on the Ahlmann Ridge.

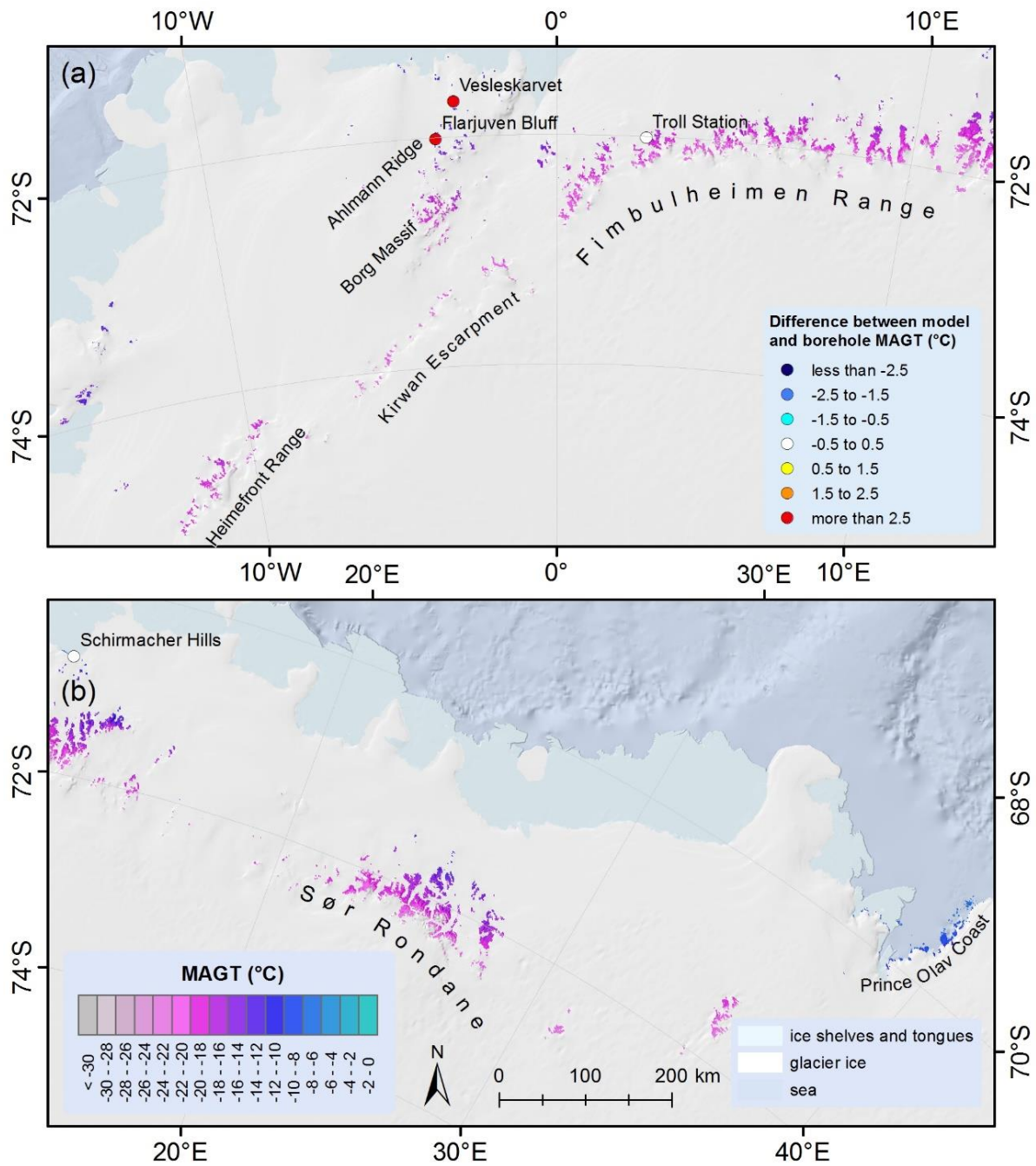


Figure 3: Permafrost temperature maps of Queen Maud Land and differences between borehole and modelled MAGT. **Legends, scale and north arrow are valid for both panels.** See Fig. 1 for location of panels (a) and (b).

3.3 Enderby Land

Permafrost occupies 14401 140 km² of ice-free area in Enderby Land, which is predominantly mountain tops and a few coastal sites. The modelled average MAGT was -11.7 °C, ranging from -22.4 °C, on summits exceeding 2000 2 000 m elevation, to -6.3 °C in the northwest part of the coast (Fig. 4). The MAGT was modelled as around -8 °C at along the majority of the coast and around -10 °C in the coastal areas of the Nye, Scott, and Tula Mountains, dropping below -15 °C at elevations exceeding 1000 m a.s.l. In in the Framnes Mountains, MAGT was modelled at between -17 and -12 °C.

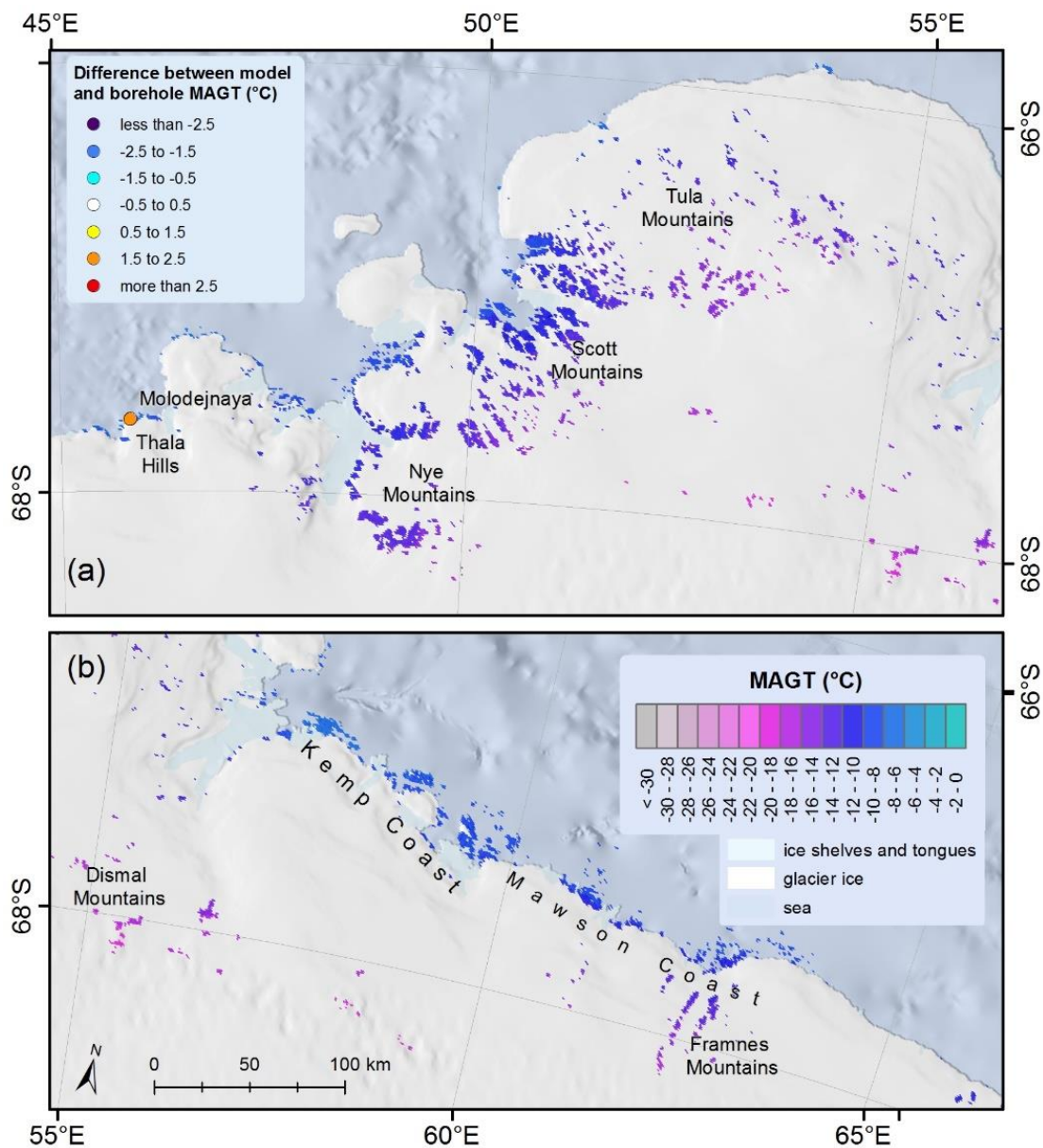


Figure 4: Permafrost temperature maps of Enderby Land and differences between borehole and modelled MAGT. Legends, scale and north arrow are valid for both panels. See Fig. 1 for location of panels (a) and (b).

3.4 Vestfold Hills

The ice-free area of the Vestfold Hills region is 27502 750 km². The modelling showed an average MAGT of -17.4 °C in this region. The MAGT ranged from -6.6 °C on the islands of the Ingrid Christensen Coast to -28.3 °C in the highest parts of the Prince Charles Mountains (Fig. 5). The MAGT in Amery Oasis, which is a part of the Prince Charles Mountains, was modelled as -13 °C, in the lowest-lying areas, down to -18 °C at elevations approaching 1000 m a.s.l. At ~~the~~ similar elevations on the Mawson Escarpment significantly lower MAGTs, from -19 °C at 200 m a.s.l down to -24 °C at 1500 m a.s.l, were recognised. In the coastal lowland areas of the Larsemann and Vestfold Hills the MAGT ranged between -10 to -7 °C.

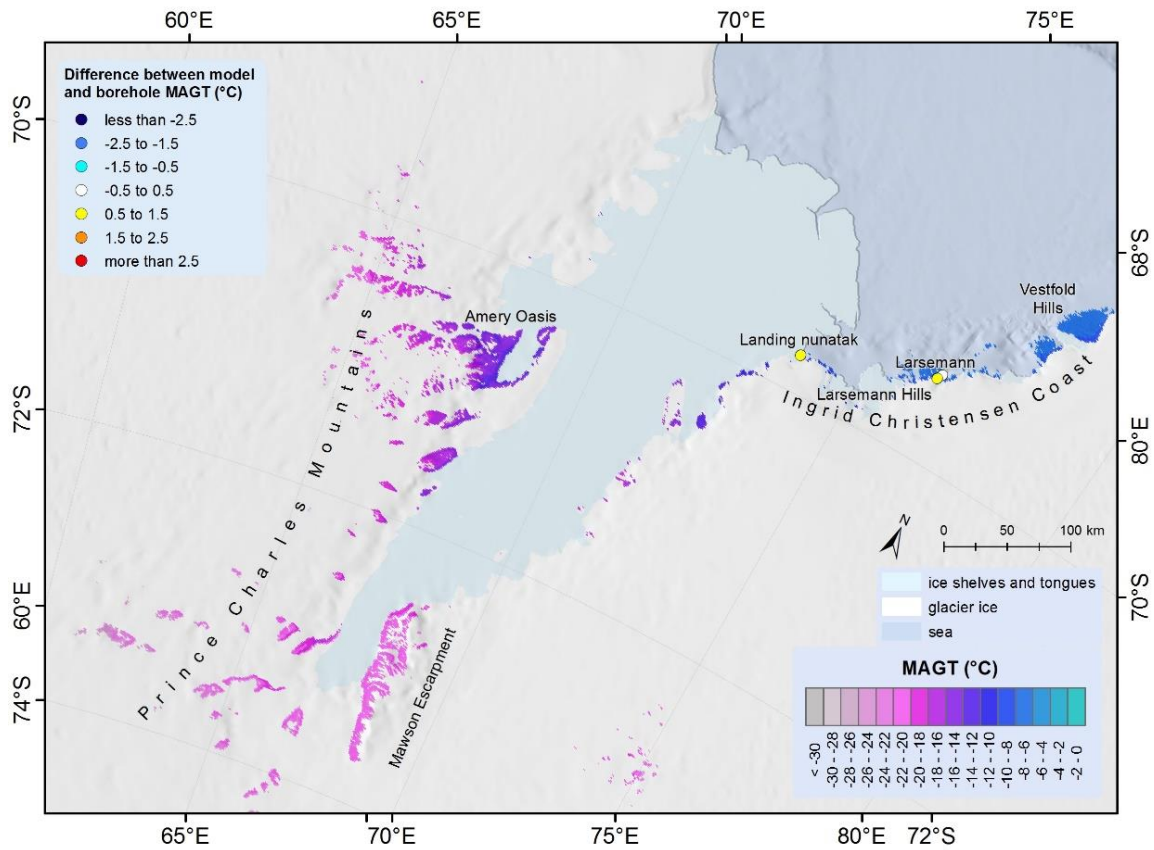


Figure 5: Permafrost temperature map of the Vestfold Hills and differences between borehole and modelled MAGT.

3.5 Wilkes Land

The majority of the 400 km² of ice free area in Wilkes Land lies in the area surrounding the Bunger Hills, where MAGTs of around -9°C were modelled close to the Shackleton Ice Shelf. The lowest MAGT of -15.9 °C was modelled on the adjacent mountains at ~~1300~~ 1300 m elevation (Fig. 6). Modelled MAGTs were -8 to -6 °C at the Budd Coast, -8 °C at the Adélie Coast, and -10 to -11 °C at the George V Coast. Due to the prevalence of low-lying regions the mean MAGT of the region was only -8.9 °C.

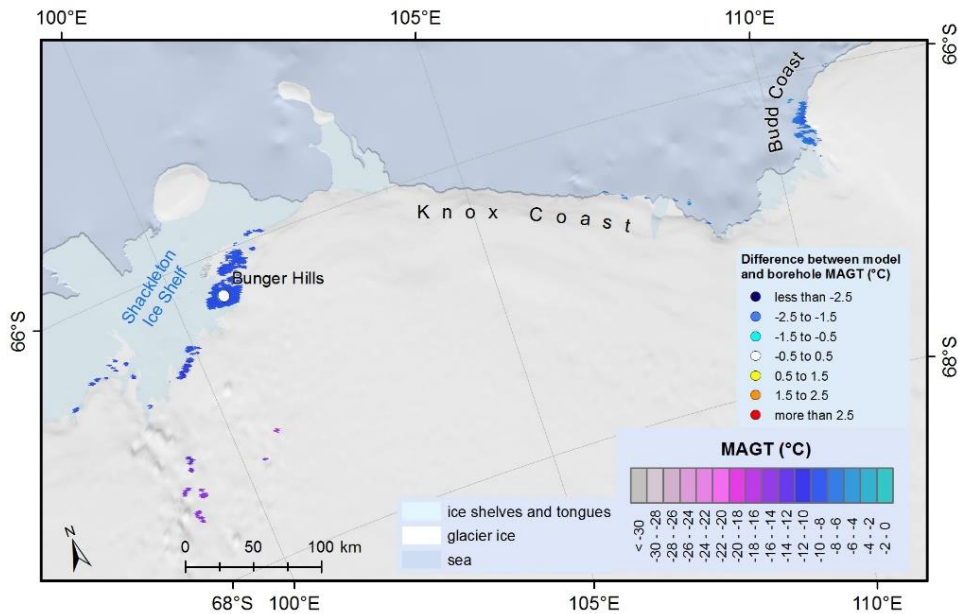


Figure 6: Permafrost temperature maps of Wilkes Land and differences between borehole and modelled MAGT. See Fig. 1 for location.

3.6 Transantarctic Mountains

The Transantarctic Mountains are the largest ice-free region, comprising 19 750 km² and extending from Cape Adare to Coats Land. The part west of the 90° meridian (Fig. 7) consists of mountain ranges mostly lower than 2000 m (except for the Thiel Mountains) that don't extend to the sea level. The highest MAGT_s of -17.0 °C_s was modelled at the foot of the Shackleton Range and at the Pensacola Mountains. The MAGTs decreased down to -29 °C in the high mountains. The lowest MAGT of -29.8 °C was modelled in the Thiel Mountains.

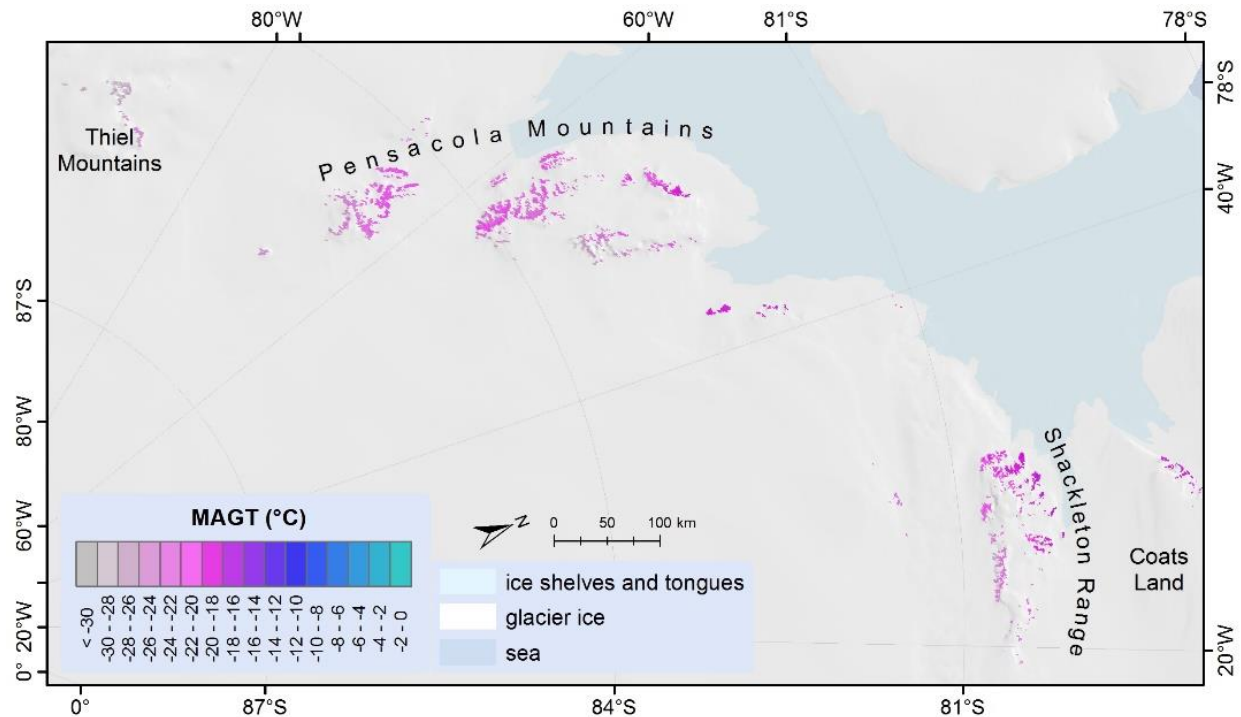


Figure 7: Permafrost temperature map of the Transantarctic Mountains west of the 90° meridian. See Fig. 1 for location.

The region east of ~~the 90° meridian~~90°E (Fig. 8) consists of numerous mountain ranges extending from the Ross Ice Shelf and Ross Sea up to more than 4000 m elevation and from 8569° S to 6985° S latitude. The results show the widest range of MAGTs among all the regions with the lowest temperature of -33.5 °C at Mount Markham in ~~the~~ Queen Elizabeth Range ~~and the warmest at~~ -8.5 °C on the Oates Coast. The modelled MAGTs close to the Ross Ice Shelf decreased northwards from -15 °C at the Amundsen Coast to -18 °C at the north of the Dufek Coast. Similar MAGTs, of between -19 and -17 °C were modelled further north along the ice shelf at the Shackleton and Hillary Coasts. Similar decreases in MAGT at higher elevations in the northward direction were observed, but local MAGT variations in relation to altitude were considerable. However, MAGTs below -30 °C were modelled at the highest parts of the mountain ranges along the Ross Ice Shelf. Higher MAGTs were modelled along the Ross Sea and range between -15 °C and -12 °C along the Scott and Borchgrevink Coasts. The modelled MAGTs were around -10 °C at Cape Adare and between -13 and -10 °C on the Pennell Coast. MAGT was modelled down to -26 °C in the Prince Albert Mountains at elevations above 2000 m a.s.l. They approach -30 °C at the highest elevations, that exceed 3000 m a.s.l., in the Deep Freeze Range. Despite the elevations reaching 4000 m a.s.l in the Admiralty Mountains, the MAGT was only down to -23 °C.

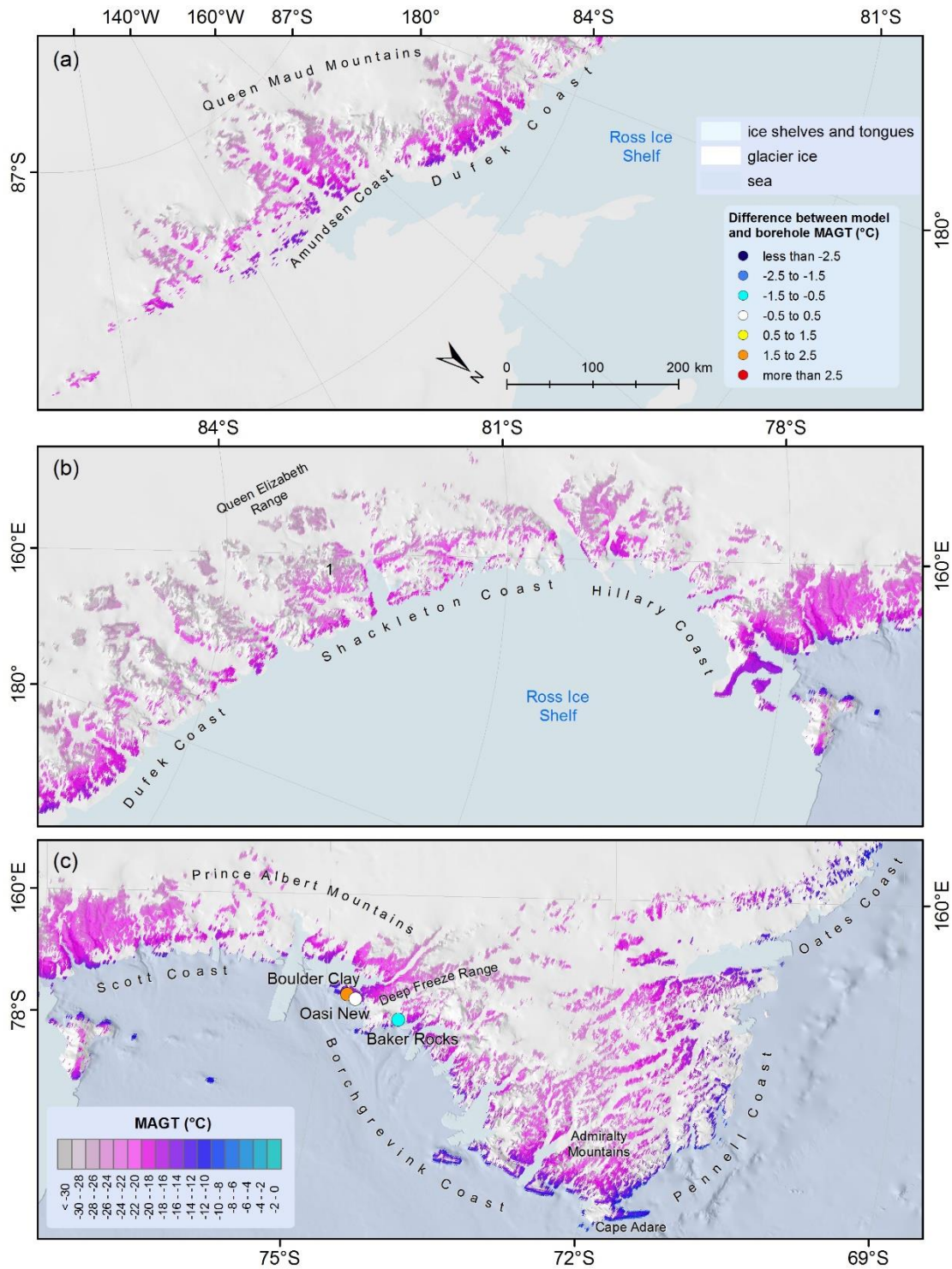


Figure 8: Permafrost temperature maps of the Transantarctic Mountains east of the 90° meridian and differences between borehole and modelled MAGT. Legends, scale and north arrow are valid for all panels. See Fig. 1 for location of panels (a), (b) and (c).

3.6.1 McMurdo Dry Valleys

The McMurdo Dry Valleys are a part of [the](#) Transantarctic Mountains ~~and~~, include a large ice-free area ([67004](#) [500](#) km²), and are one of the most extensively studied permafrost regions in Antarctica ([Levy, 2013](#); [Bockheim](#)

et al., 2007). The lowest MAGT among the dry valleys is modelled in the Victoria Valley falling below $-24\text{ }^{\circ}\text{C}$ at the lowest part (Fig. 9). A winter ground temperature inversion is pronounced with MAGTs in the surrounding valleys modelled at around $-21\text{ }^{\circ}\text{C}$. The MAGT also increases up the valleys to $-21\text{ }^{\circ}\text{C}$ in the McKelvey, Balham, and Barwick Valleys. No MAGT inversion was modelled in the Wright Valley, where MAGTs ranged between -21 and $-19\text{ }^{\circ}\text{C}$ and in the Taylor Valley, which is the warmest with MAGT of $-17\text{ }^{\circ}\text{C}$ in the lower-lying parts, and $-20\text{ }^{\circ}\text{C}$ in the upper part, of the valley. At the Olympus and Asgard Ranges and the Kukri Hills, which surround the valleys, MAGTs of between -23 and $-20\text{ }^{\circ}\text{C}$ were modelled. In the surrounding mountains, close to the ice sheet, modelled MAGTs were around $-25\text{ }^{\circ}\text{C}$ and reached $-27\text{ }^{\circ}\text{C}$ at the highest and the most east-lying mountains. MAGTs at along the coast of McMurdo Sound ranged from -13 to $-17\text{ }^{\circ}\text{C}$. On Ross Island, the MAGT was modelled teas $-16\text{ }^{\circ}\text{C}$ at the Scott and McMurdo Bases which are near sea level and down to $-24\text{ }^{\circ}\text{C}$ at higher altitudes on Mount Erebus.

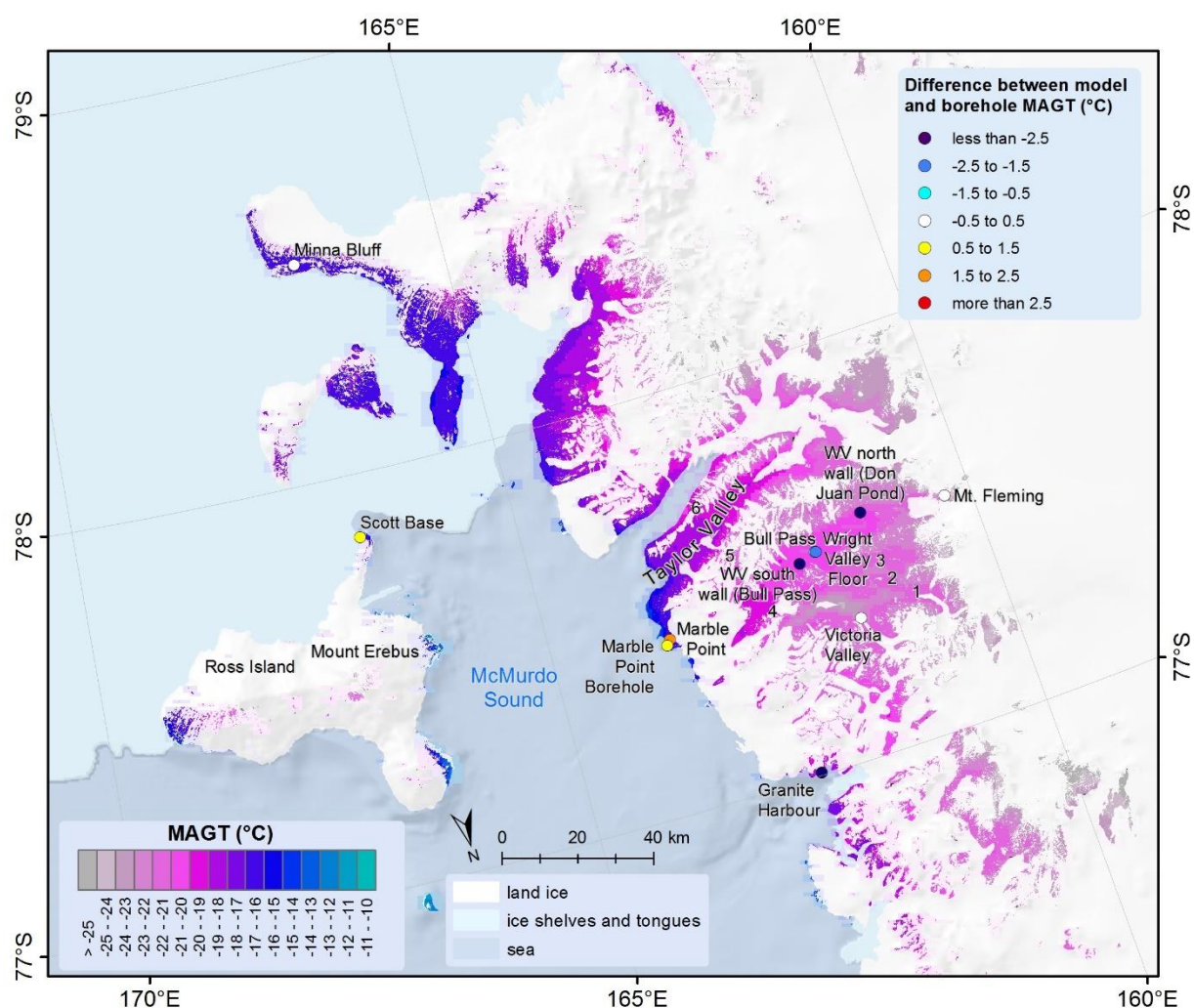


Figure 9: Permafrost temperature map of the McMurdo Dry Valleys and differences between borehole and modelled MAGT. See Fig. 1 for location. Note: the MAGT colour ramp is different from other figures. 1: McKelvey Valley; 2: Balham Valley; 3: Barwick Valley; 4: Olympus Range; 5: Asgard Range 6: Kukri Hills.

3.7 Ellsworth Mountains

The ice-free area of the Ellsworth Mountains occupies 380 km² of high-elevation terrain; ~~therefore the~~ with a modelled mean MAGT ~~was of~~ -21.5 °C. The highest temperature was modelled at the foot of the mountains (-17.4 °C) at 500 m a.s.l. with -21 °C at 1000 m a.s.l., -22 °C at 2000 m, and ~~down to~~ -26.1 °C at the highest elevations of Vinson Massif (Fig. 10).

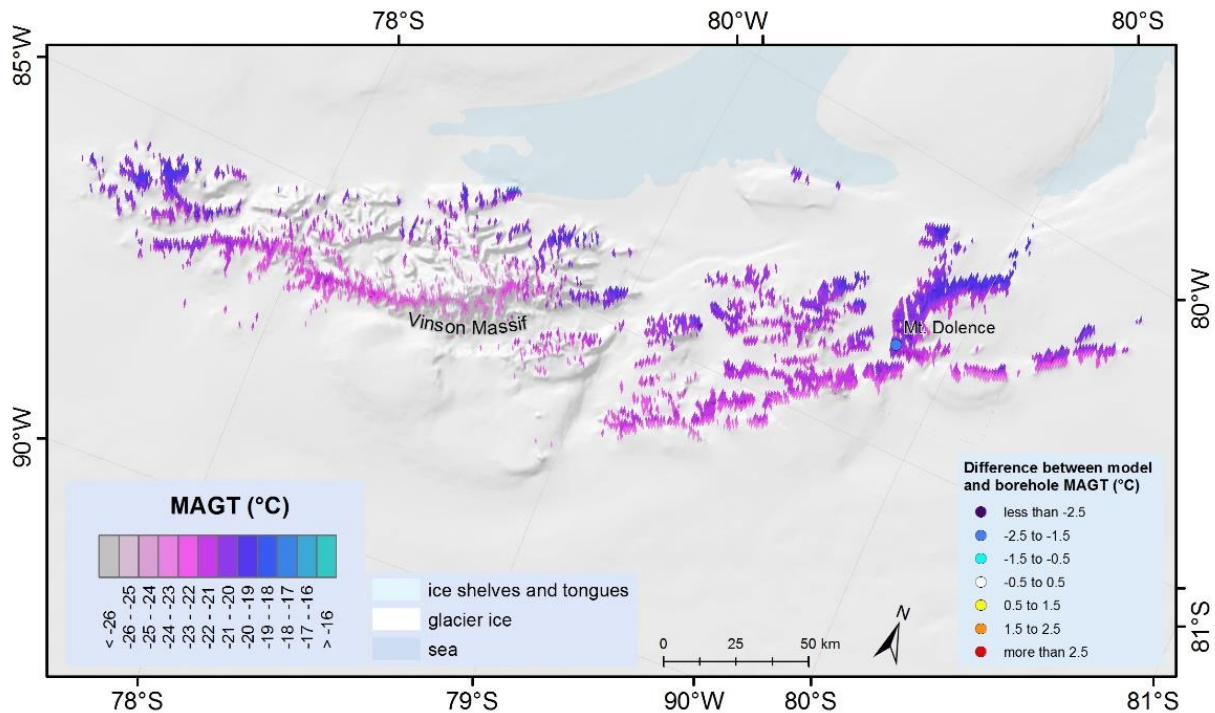
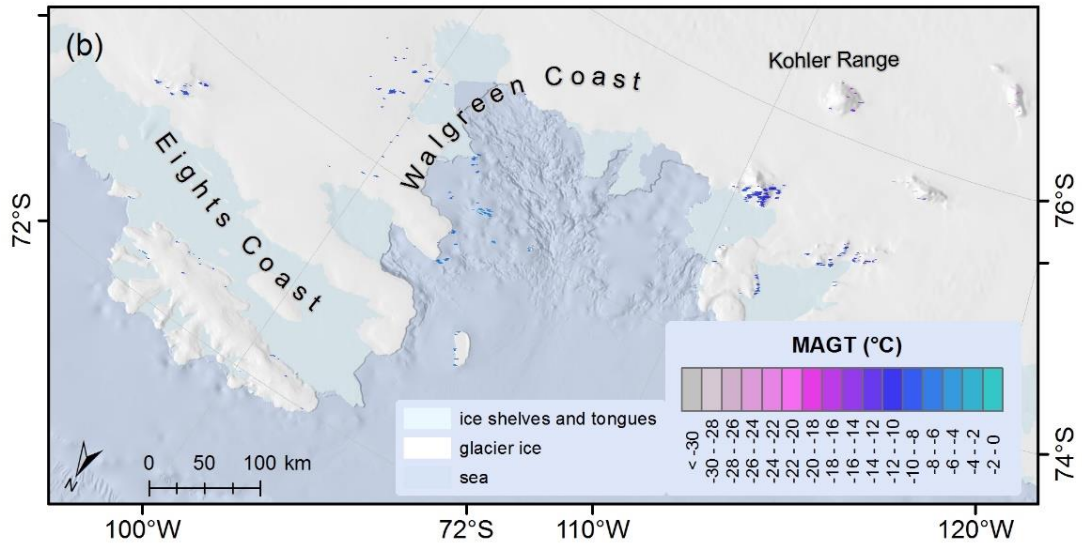
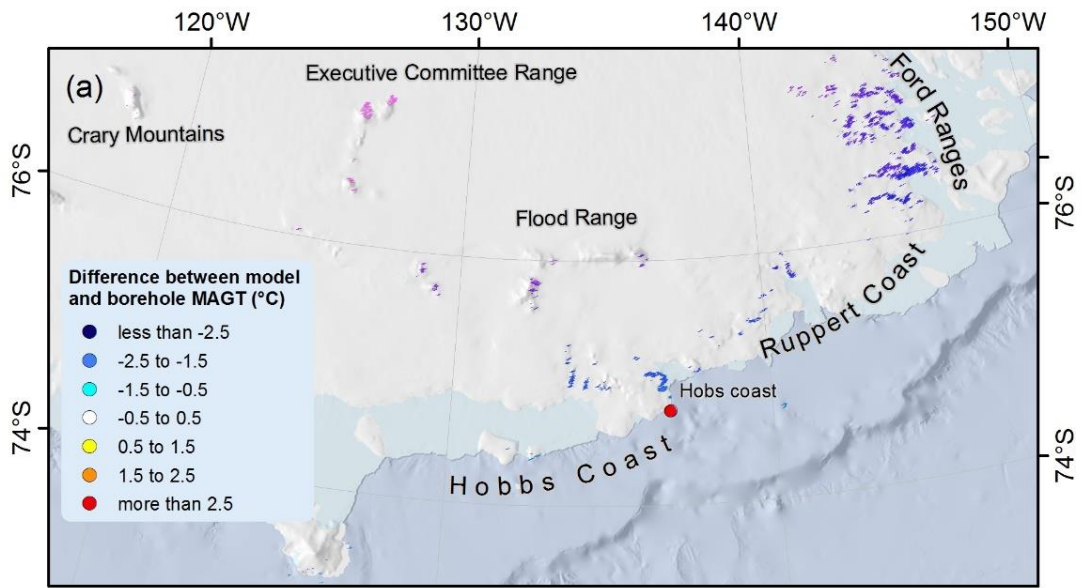


Figure 10: Permafrost temperature map of the Ellsworth Mountains and differences between borehole and modelled MAGT. See Fig. 1 for location.

3.8 Marie Byrd Land

The ice free areas in Marie Byrd Land occupy only 210 km² and consist mostly of rock outcrops at lower elevations close to the coast and volcanos protruding through the ice sheet. In the Ford Ranges, MAGT was modelled as from -10 °C close to sea level to -16 °C at elevations exceeding 1000 m a.s.l (Fig. 11). MAGTs between -11 and -8 °C were modelled at the Hobbs, Walgreen, Eights and Ruppert Coasts, reaching -6 °C on the islands surrounded by open sea. The volcano-mountain ranges reaching 3000 m a.s.l. (Flood and Kohler Range), had MAGTs typically ranging between -16 to -14 °C at their peaks. Modelled MAGTs were between -25 and -21 °C on the Executive Committee Range, where rock outcrops occur above 2000 m a.s.l. and the highest peaks extend to over 4000 m a.s.l.



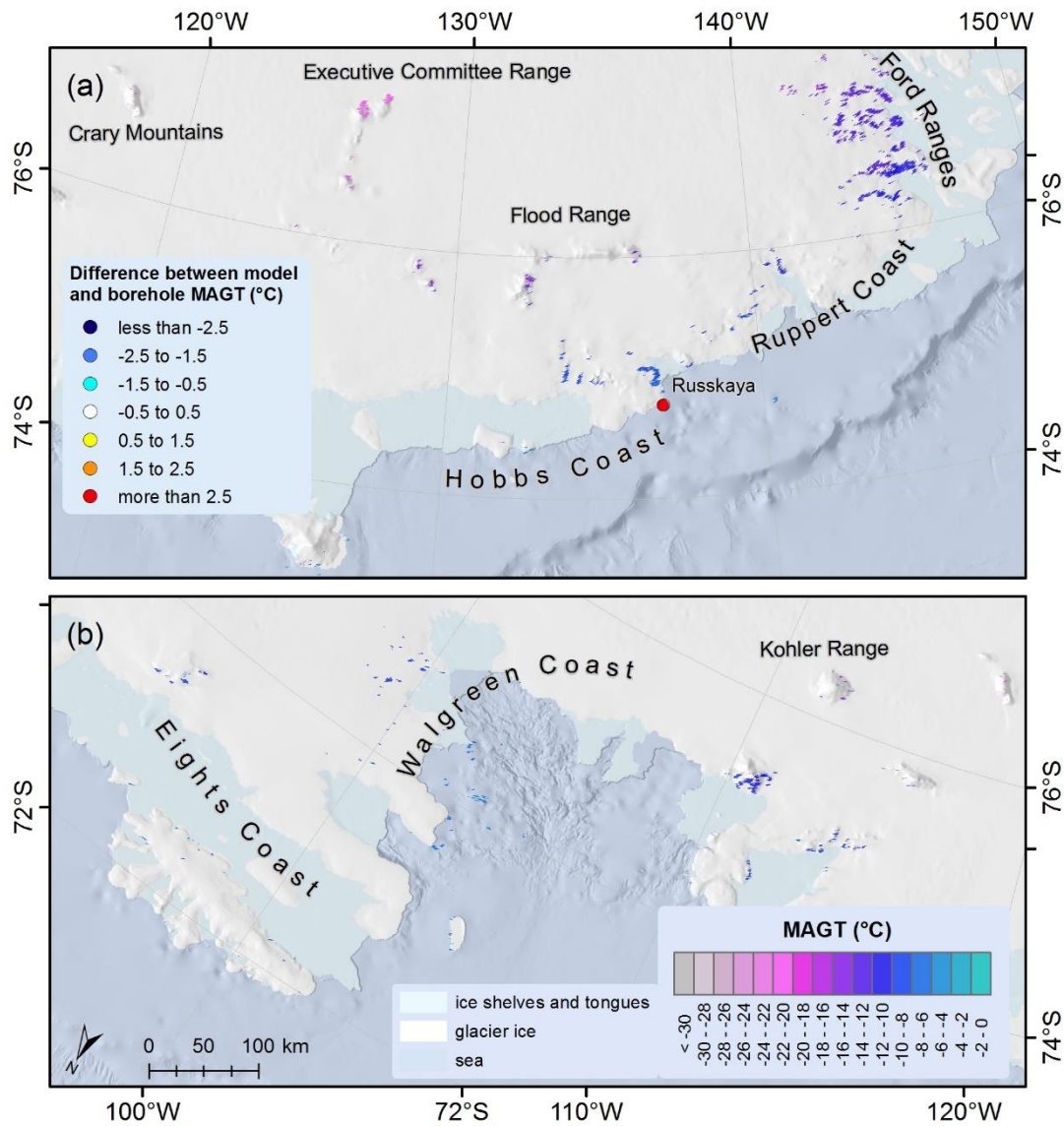


Figure 11: Permafrost temperature maps of Marie Byrd Land and differences between borehole and modelled MAGT. Legends, scale and north arrow are valid for both panels. See Fig. 1 for location of panels (a) and (b).

3.9 Antarctic Peninsula

The ice-free areas of the Antarctic Peninsula cover 3 800 km² including the South Shetland islands where the modelled MAGT was slightly below 0°C and the mountains of the south-eastern Antarctic Peninsula with modelled MAGT/MAGTs of around -19 °C. The modelled near-surface permafrost temperatures in the Antarctic Peninsula were the warmest among all Antarctic regions with an average modelled MAGT of -7.3 °C (Fig. 12).

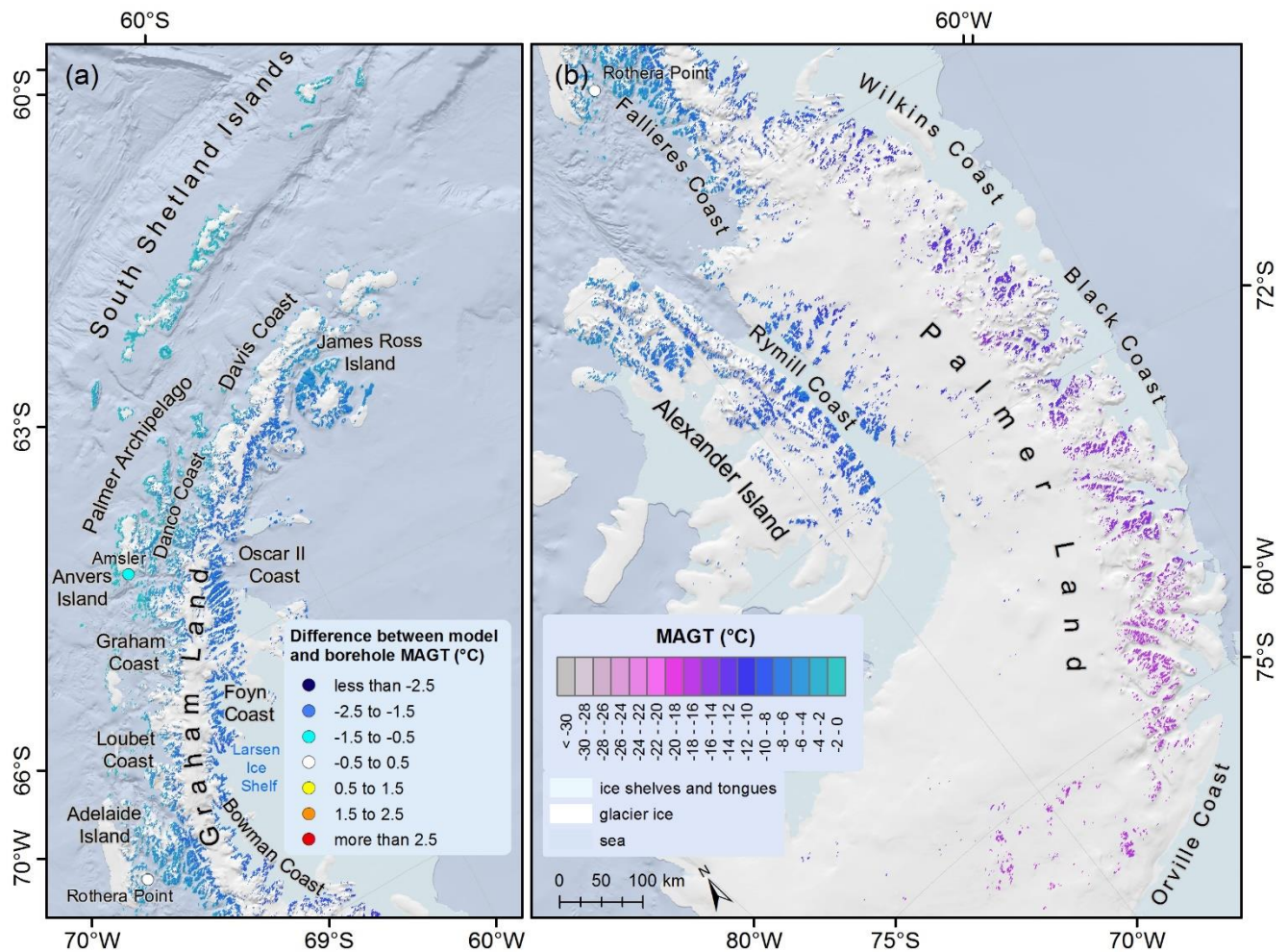


Figure 12: Permafrost temperature maps of the Antarctic Peninsula and differences between borehole and modelled MAGT. Legends, scale and north arrow are valid for both panels. See Fig. 1 for location of panels (a) and (b).

3.9.1 Palmer Land

The mountains of Palmer Land show considerable differences between the eastern and western parts of the peninsula. Modelled MAGTs at the mountains of the Orville Coast were around $-17\text{ }^{\circ}\text{C}$, increasing to about -12 to $-15\text{ }^{\circ}\text{C}$ at the Black Coast and eventually rising above $-10\text{ }^{\circ}\text{C}$ at the Wilkins Coast. On the west side at the Fallieres Coast MAGTs of up to $-4\text{ }^{\circ}\text{C}$ were modelled. Temperatures decreased to -6 to $-8\text{ }^{\circ}\text{C}$ at the Rymill Coast, around $-10\text{ }^{\circ}\text{C}$ at 1000 m a.s.l. , and approached $-12\text{ }^{\circ}\text{C}$ at 1500 m a.s.l. . Similar MAGT ranges were modelled on Alexander Island where MAGTs close to the coast were around $-5\text{ }^{\circ}\text{C}$, decreasing to between -9 and $-7\text{ }^{\circ}\text{C}$ at 1000 m a.s.l. and falling below $-10\text{ }^{\circ}\text{C}$ at elevations above 2000 m a.s.l.

3.9.2 Graham Land

A considerable increase in modelled MAGT from the east to the west of Graham Land was observed, where the south part of the east coast is protected by the Larsen Ice Shelf. Ground temperatures gradually increased in the northward direction on both sides of the peninsula. MAGTs at the Bowman and Foyn Coasts ranged between -8 and $-6\text{ }^{\circ}\text{C}$ and slowly increased from $-6\text{ }^{\circ}\text{C}$ at the Oscar II Coast to around $-4\text{ }^{\circ}\text{C}$ at the northern-most part of the

mainland although still falling below $-8\text{ }^{\circ}\text{C}$ at higher elevations. On the west side, MAGT gradually decreased from around $-2\text{ }^{\circ}\text{C}$ in the north Davis Coast to $-5\text{ }^{\circ}\text{C}$ at the south of the Danco Coast and Anvers Island, where MAGT also fell below $-6\text{ }^{\circ}\text{C}$ at higher elevations. Similar MAGT ranges were observed at the Graham and Loubet Coasts and at Adelaide Island but were lower than $-7\text{ }^{\circ}\text{C}$ at higher elevations. Small Islands along the west coast of the Antarctic Peninsula had a modelled MAGT of between -3 and $-1\text{ }^{\circ}\text{C}$.

3.9.3 South Shetland Islands and James Ross Island

Another frequently studied area in the Antarctic is the Northern Antarctic Peninsula, especially the South Shetland Islands. At sites close to sea level, the modelled MAGT was usually above $-1\text{ }^{\circ}\text{C}$ on the South Shetland Islands (Fig. 13). MAGT decreased below $-2\text{ }^{\circ}\text{C}$ on sites that are not adjacent to the coast but still low-lying such as Byers and Hurd Peninsulas on Livingston Island and Fildes Peninsula on King George Island. The MAGT was below $-4\text{ }^{\circ}\text{C}$ on the highest unglaciated peaks of Livingston and Smith Islands and reached $-3\text{ }^{\circ}\text{C}$ on Deception Island.

Modelled MAGTs were ~~significantly~~noticeably colder on James Ross Island than on the South Shetland Islands, and, at sites adjacent to the sea, ranging from $-3\text{ }^{\circ}\text{C}$ in the north down to $-5\text{ }^{\circ}\text{C}$ in the south. Lower lying ice-free areas, including Seymour Island, had MAGTs typically between -6 and $-5\text{ }^{\circ}\text{C}$. The MAGTs on the highest rock outcrops were modelled as down to $-7\text{ }^{\circ}\text{C}$.

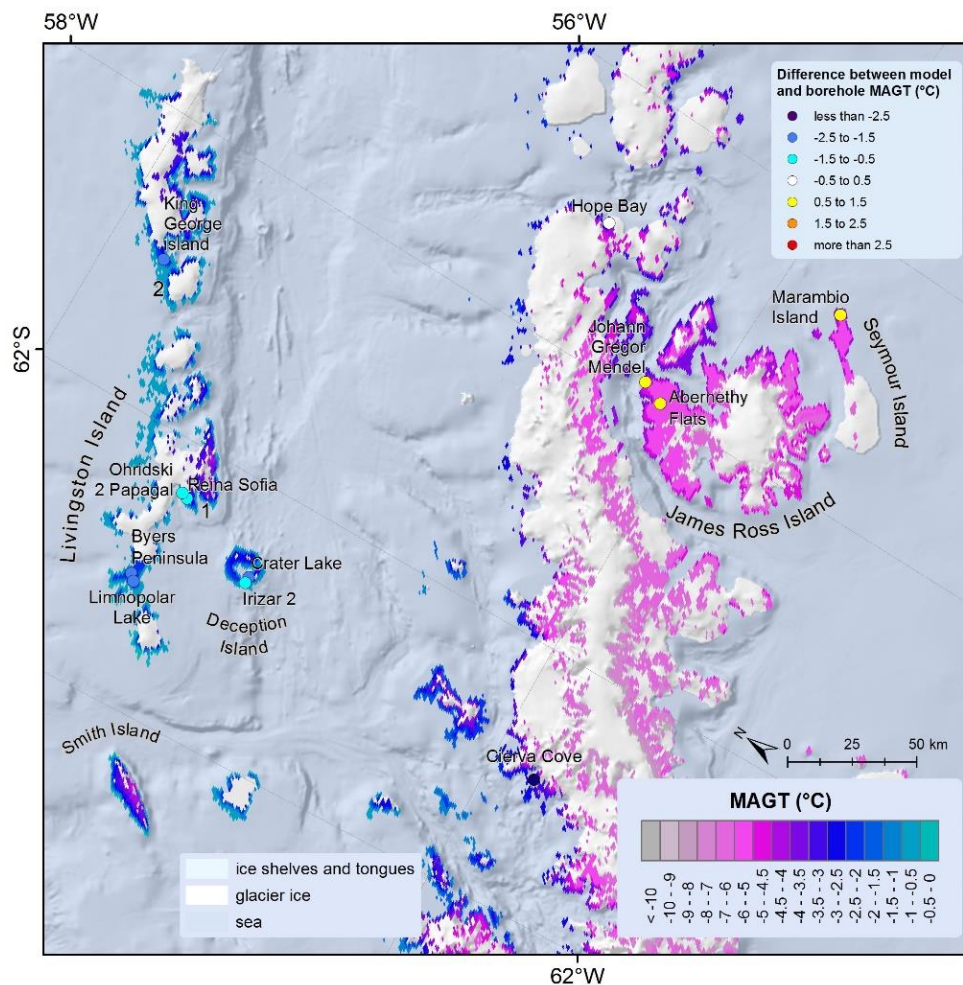
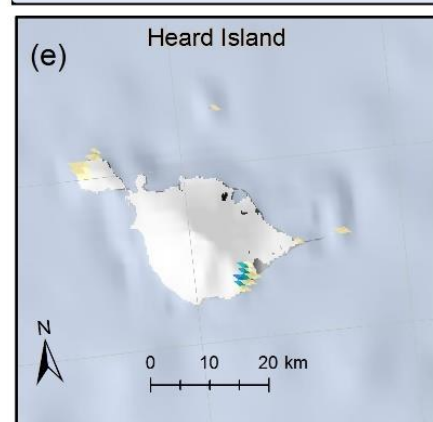
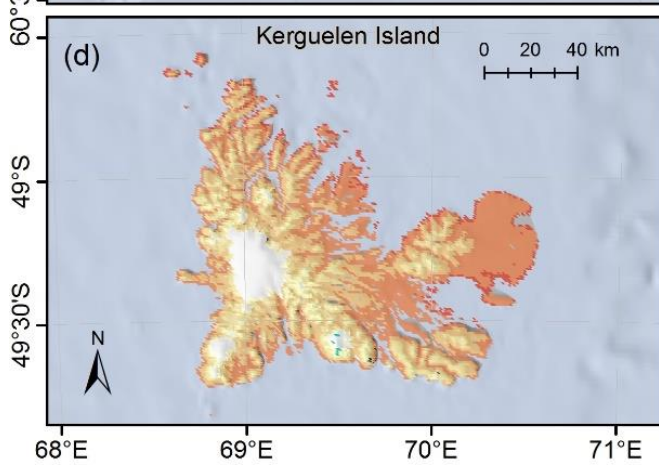
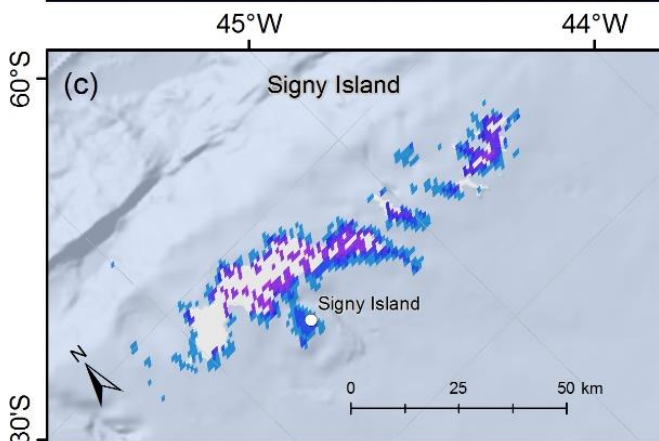
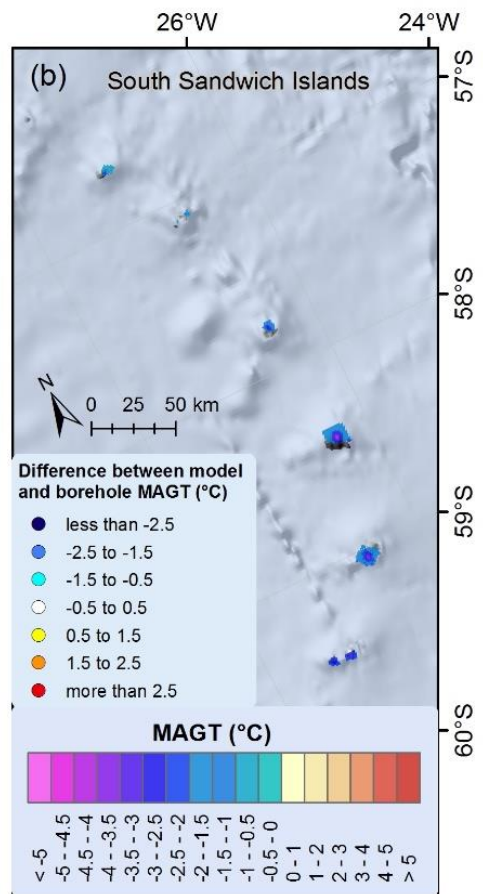
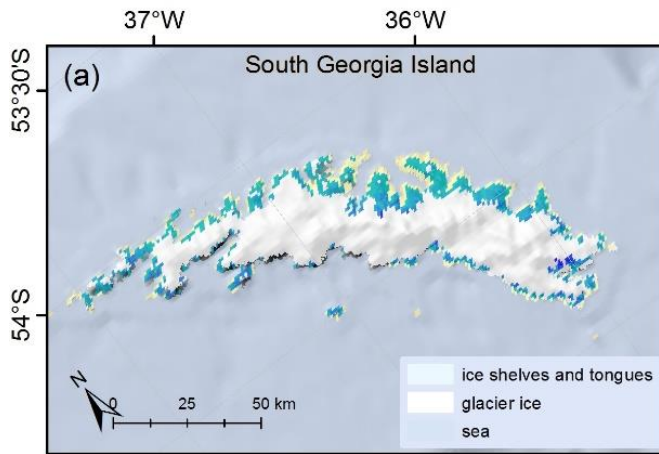


Figure 13: Permafrost temperature map of the Northern Antarctic Peninsula and differences between borehole and modelled MAGT. –See Fig. 1 for location. Note: the MAGT colour ramp is different from other figures. 1: Hurd Peninsula; 2: Fildes Peninsula.

3.10 Other Antarctic and sub-Antarctic Islands

The modelling results were derived for the Antarctic Islands and sub-Antarctic Islands where the size and ice-free area of the island is sufficient that MODIS LST data were available. MAGT on Signy Island ranged from -1.5 °C at the coast to -4 °C in the interior. Permafrost was modelled on all South Sandwich Islands with similar MAGT ranges to those on Signy Island (Fig. 14). Less permafrost is modelled on South Georgia Island, where MAGTs at the coast increase to ± 1 °C and sporadic permafrost starts to occur at elevations above 100 m. The MAGTs decreased below -2 °C at the highest-lying rock outcrops. No permafrost was modelled on the Crozet Islands. MAGTs below 0 °C were modelled at the highest elevations of Kerguelen Island and in isolated permafrost patches occurring above 500 m a.s.l. Permafrost is present also on the southern-most ice-free area of Heard Island.



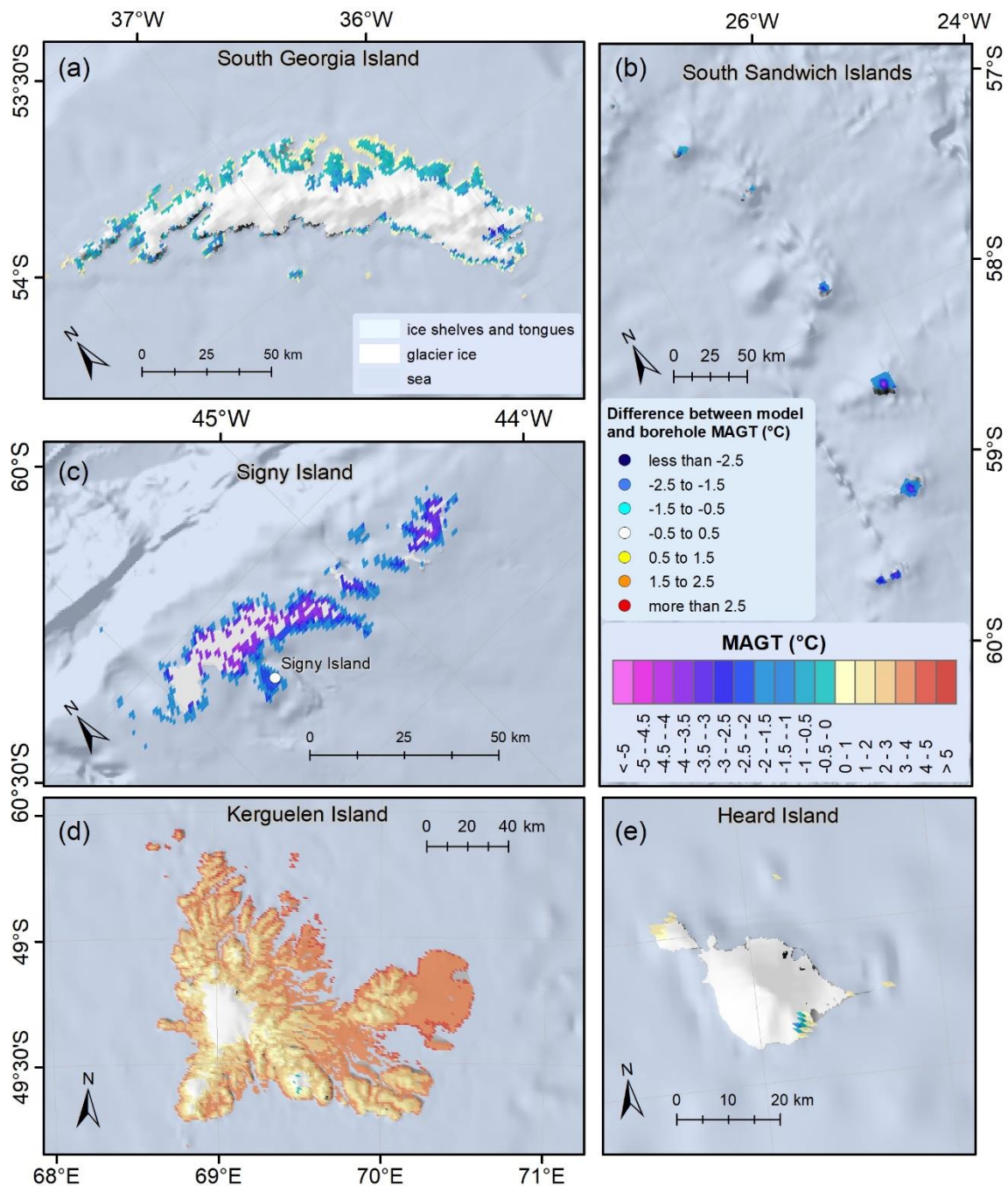


Figure 14: Permafrost temperature maps of Antarctic Islands and difference between borehole and modelled MAGT. Legends are valid for all panels. See Fig. 1 for location of panels (a), (b), (c), (d) and (e). Note: the MAGT colour ramp is different from other figures.

3.11 Regional MAGT distribution

The MAGT distribution of Antarctic is bimodal with the most pronounced peak at $-21\text{ }^{\circ}\text{C}$ and the second peak at $-7\text{ }^{\circ}\text{C}$ (Fig. 15). The peaks correspond to the two largest ice-free areas of the Transantarctic Mountains and the Antarctic Peninsula, however the temperatures around the $-20\text{ }^{\circ}\text{C}$ peak also occur in other regions such as Queen Maud Land, the Vestfold Hills and the Ellsworth Mountains. The most commonly modelled temperatures were

between -23 and -18 °C and usually occurred in the mountains rising above the Antarctic Ice-sheet and glaciers. MAGTs of between -10 and -6 °C occurred in the coastal areas of Wilkes Land, Marie Byrd Land, Queen Maud Land, Enderby Land, and the Vestfold Hills, ~~but~~. However the peak of temperature distribution at coastal sites shifted towards -7 °C because of MAGTs on the Antarctic Peninsula. The peak of coastal areas would be at -9 °C if the Antarctic Peninsula was excluded.

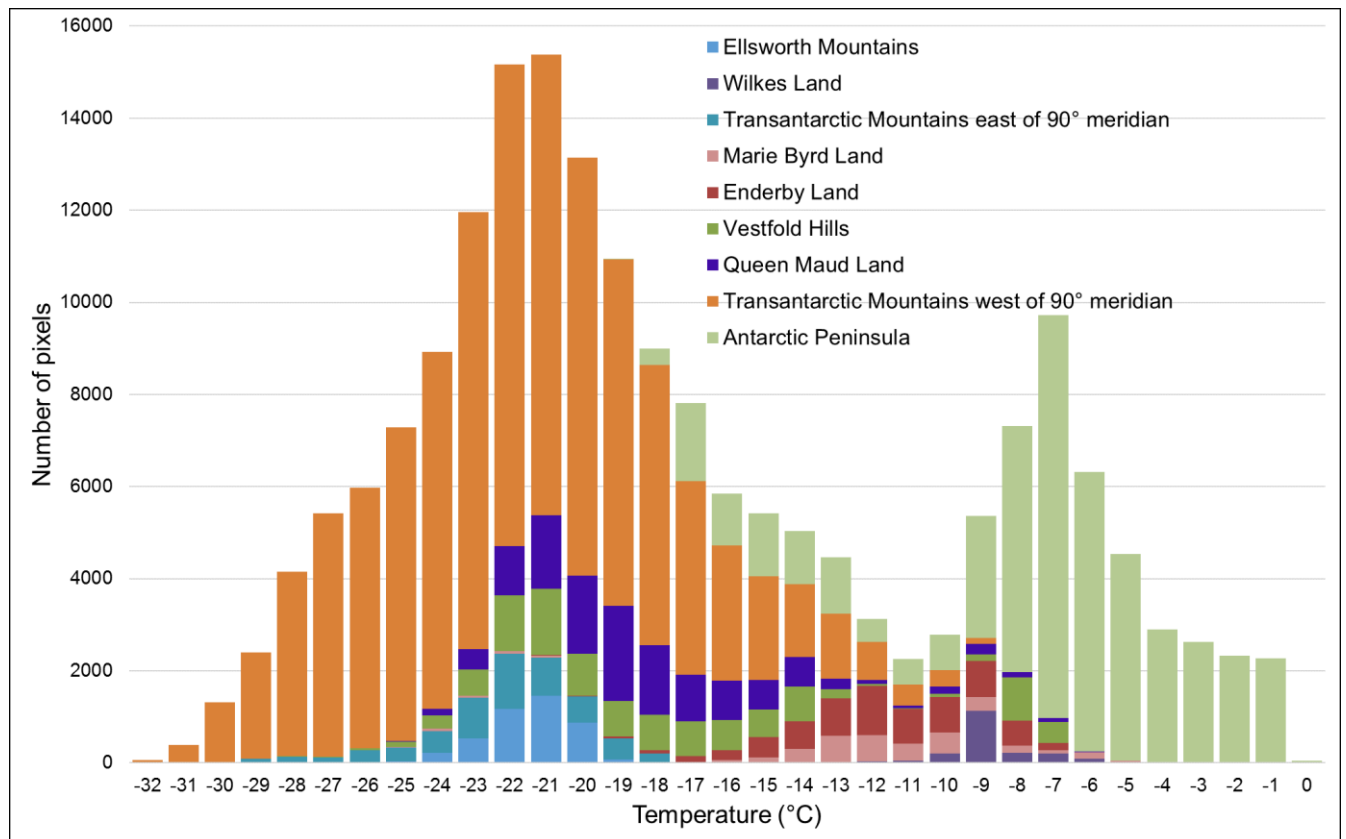


Figure 15: Histogram of temperature distribution across the Antarctic for 1 °C bins. Note: The ice-free areas were often smaller than the analysed pixel size.

3.12 Altitudinal MAGT gradients

Average MAGT lapse rate for the whole Antarctic was $0.40 \text{ } ^\circ\text{C } 100 \text{ m}^{-1}$ ranging from $0.15 \text{ } ^\circ\text{C } 100 \text{ m}^{-1}$ in the Ellsworth Mountains to $0.59 \text{ } ^\circ\text{C } 100 \text{ m}^{-1}$ in Enderby Land. The lapse rates increased from $0.21 \text{ } ^\circ\text{C } 100 \text{ m}^{-1}$ in Wilkes Land to $0.38 \text{ } ^\circ\text{C } 100 \text{ m}^{-1}$ in the Transantarctic Mountains, $0.44 \text{ } ^\circ\text{C } 100 \text{ m}^{-1}$ in the Vestfold Hills, $0.47 \text{ } ^\circ\text{C } 100 \text{ m}^{-1}$ in Marie Byrd Land and in the Antarctic Peninsula to $0.49 \text{ } ^\circ\text{C } 100 \text{ m}^{-1}$ in Queen Maud Land.

The lapse rates ~~are is indicating indicate~~ significant regional differences in the modelled MAGT patterns in relation to elevation (Fig. 16). The warmest among all regions was the Antarctic Peninsula which had MAGTs similar to Marie Byrd Land ~~of -12 °C only~~ at around ~~-12 °C between~~ 1300 m a.s.l., ~~which is again colder at higher elevations~~. Marie Byrd Land, Queen Maud Land, Enderby Land and Wilkes Land had MAGTs of -9 °C at the coast but show varying characteristics of temperature decrease with elevation. Marie Byrd Land was the warmest with a decrease in MAGT up to 1500 m a.s.l., and a faster decrease to -25 °C at 3000 m a.s.l. The

slower decrease in temperature with altitude to the ~~1500m~~1500 m elevation was also modelled in Enderby Land but the MAGT was colder. The MAGT decreased rapidly to -13 °C at 700 m a.s.l. in Queen Maud Land, where it slightly increased with elevation and then dropped steadily to -22 °C at 2800 m a.s.l. The MAGT increase with elevation could be explained by presence of rock outcrops with similar elevation in different latitudes or in different settings regarding continentality.

The modelled MAGT in the Vestfold Hills dropped rapidly from -10 °C at the coast to -17 °C at 200 m a. s. l. and then gradually decreased to -24 °C at 2000 m a.s.l. There are no rock outcrops close to sea level in the Ellsworth Mountains and the MAGT at 100 m a.s.l. was -20 °C. In the Ellsworth Mountains there was a slow decrease of the modelled MAGT, to -25 °C at 3000 m a. s. l. The coldest MAGTs (below -30 °C) were modelled in the Transantarctic Mountains. In the part west of the 90 ° meridian, the MAGT dropped from -20 °C at 500 m a.s.l to -27 °C at 2000 m a.s.l. but the absolute temperatures were lower east of the 90 ° meridian where elevations exceed 4000 m a.s.l.

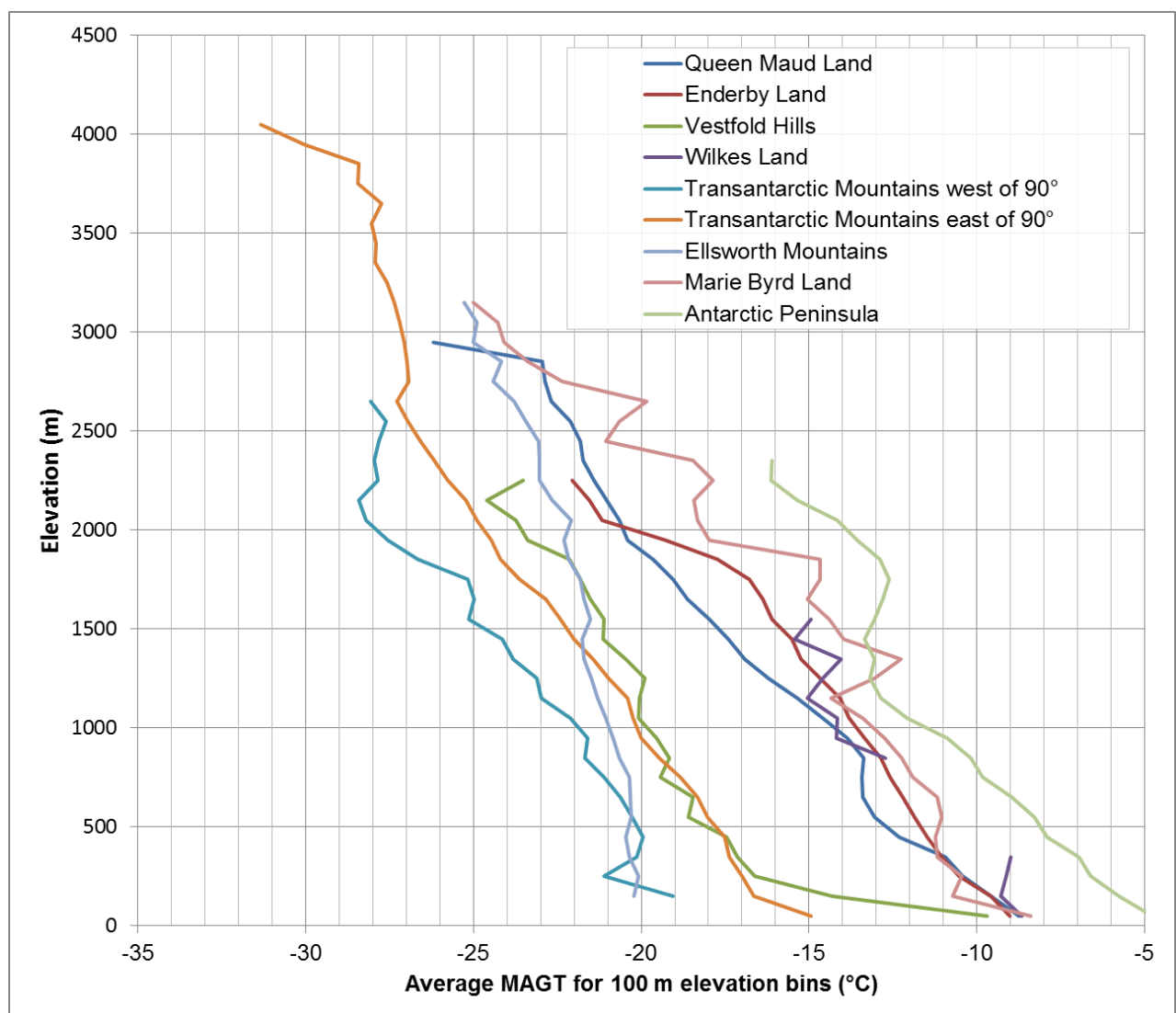


Figure 16: Altitudinal MAGT gradients for Antarctic Soil Regions calculated for 100 m elevation bins.

According to the gradients for sub-regions of the Northern Antarctic Peninsula, the warmest were the South Shetland Islands followed by Palmer Archipelago (Fig. 17). The altitudinal MAGT profiles showed clear differences between the western and eastern parts of the Northern Antarctic Peninsula mainland, although James Ross Island had a similar altitudinal profile to the West Antarctic Peninsula mainland. A significant decrease in MAGT from sea level to 100 m elevation was observed on the South Shetland Islands, Palmer Archipelago, and on the West Antarctic Peninsula mainland.

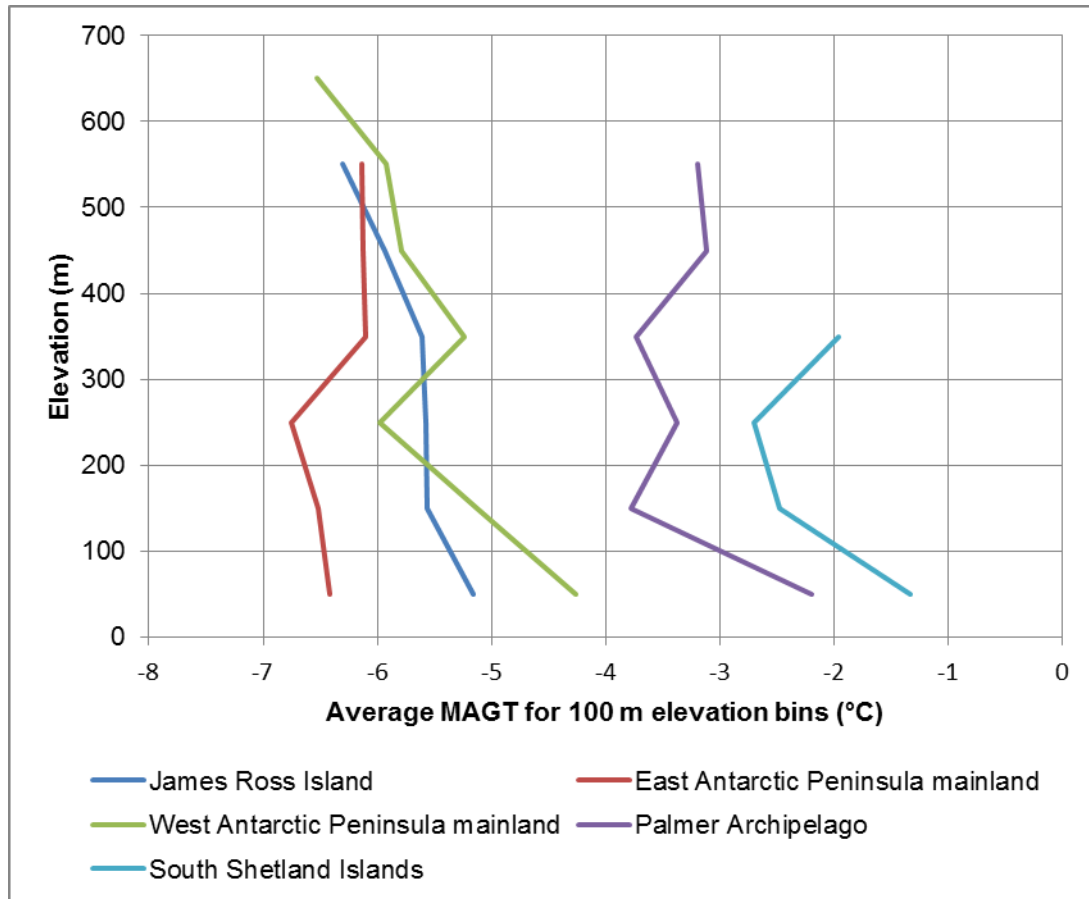


Figure 17: Altitudinal MAGT gradients for the Northern Antarctic Peninsula calculated for 100 m elevation bins.

4 Discussion

4.1 Comparison to borehole measurements

4.1.1 Queen Maud Land

The modelled MAGT ~~is~~was, according to validation data, ~~was~~ over-estimated in Queen Maud Land- (Fig. 3). Over-estimation in Schirmacher Hills and Troll Station was below 1 °C but was higher than 4 °C in Flarjuven Bluff and Vesleskarvet. Both stations are located on nunataks, which are exposed to wind that blows ~~away~~ the snow away. The estimated 120 mm of annual snowfall resulted in ~~too low~~ n_f -factors that were too low for snow-free conditions. However, the minimum MAGT of the ensemble spread approaches the measured MAGT at both stations (Appendix A).

4.1.2 Enderby Land, Vestfold Hills and Wilkes Land

The borehole data in Enderby Land were from the Molodejnaya station (Thala Hills), where modelled MAGT was over-estimated by 1.6 °C- (Fig. 4). The over-estimation can be explained by rather thin snow cover due to strong winds and snow redistribution at the borehole site, which is confirmed by small differences between measured winter air and ground surface temperatures. The MAGT ~~is~~was accurately modelled in the coastal parts of the Vestfold Hills region, where validation data ~~are~~were available- (Fig. 5). The difference between modelled and measured MAGT ~~is~~was small at the Larsemann Hills borehole but slight MAGT over-estimation (between 0.6 and 0.9 °C) was observed in comparison to the Larsemann and Landing Nunatak borehole measurements. Similarly, the MAGT was accurately modelled at the Bunger Hills station in the Wilkes Land region, with only small differences in comparison to measured ground temperature- (Fig. 6).

4.1.3 Transantarctic Mountains

The majority of the available validation data in the Transantarctic Mountains region ~~is available~~was in the vicinity of the McMurdo Dry Valleys- (Fig. 9). The sites on the floors of the McMurdo Dry Valleys (Victoria Valley, Wright Valley Floor, and Bull Pass) were modelled well with slight over-estimation in Victoria Valley and under-estimation of around 1 °C in the Wright Valley. Two observation sites on small terraces on the walls of the Wright Valley (WV south wall and WV north wall) were modelled 3–4 °C too cold. The difference can be explained by the micro-location of the both sites, which are sheltered from katabatic winds, are above the winter inversion layer, and receive abundant summer solar radiation. The MAGT was over-estimated by up to 1 °C at Mt. Fleming, Scott Base, and the Marble Point Borehole, which lie outside the valleys. The MAGT at the Marble Point site, characterised by glacial till, was over-estimated by 2.2 °C, however, the Marble Point Borehole, which was drilled in granite bedrock approx. 1 km away, showed smaller over-estimation. The MAGT was under-estimated by more than 4 °C at the Granite Harbour site which has a warm microclimate as it is situated on north-facing moraine that receives a lot of meltwater from up-slope.

Outside the McMurdo Dry Valleys, MAGT measurements from the Zucchelli Station and Baker Rocks ~~are~~were available- (Fig. 9). The MAGT ~~is~~was over-estimated by 2.3 °C at the Boulder clay borehole, which was drilled in a glacial till, exposed to katabatic winds, and characterised by numerous snow drifts (Guglielmin, 2006) ~~which causes~~causing high local variability in permafrost conditions. On the other hand, the MAGT was over-estimated by only 0.2 °C at the Oasi New borehole, which is located in a granitic outcrop. MAGT at the Baker Rocks site, which is situated in littoral deposits (Raffi and Stenni, 2011), was under-estimated by 0.9 °C.

4.1.4 Marie Byrd Land

The only available borehole data in Marie Byrd Land ~~is~~(Fig. 11) was from the Russian research station Russkaya (the name of the borehole is Hobbs coast)-. According to the measured MAGT between 2008–2013 the modelled MAGT ~~is~~was over-estimated by 3.4 °C. The area is characterised by frequent storms and ~~very~~ strong winds, which blow off most of the snow on one hand and decrease the number and quality of the MODIS measurements on the other hand. The snow free-conditions at the Hobbs coast borehole site were likely not simulated by the snow model, which resulted in the MAGT over-estimation. An alternative explanation could be the measurement

period, which ~~is~~was only five years in comparison to 17 modelled years. No validation data were available for the higher elevations of the volcanic ranges. The modelled MAGTs there might be under-estimated because the TTOP model doesn't account for the ground heat flux. This can especially be the case in the locations with recent volcanic activity.

4.1.5 Antarctic Peninsula

Comparison of the modelled MAGT with measured MAGT in boreholes showed an under-estimation in the Western Antarctic Peninsula and slight over-estimation in the Eastern Antarctic Peninsula. (Fig. 13). The MAGTs are under-estimated by between 1 and 2.1 °C on the South Shetland Islands (King George, Livingston and Deception Island). ~~These~~The under-estimations may be explained by heat advection from meltwater and rain that is not simulated by the model but is especially common in this part of the Antarctic. Another possible explanation for deviations of the modelled MAGT in the north-eastern Antarctic Peninsula are the frequent cloudy conditions. Although clouds are generally masked out from the MODIS LST and replaced by ERA Reanalysis temperatures, measurements in some areas are still contaminated with cloud temperatures, which results in MAGT under-estimation (Østby et al., 2014).

Recent shallowing of thaw depth and ground cooling were observed on Deception Island by Ramos et al. (2017). However, similar cooling was recorded also in the Eastern Antarctic Peninsula, but MAGT was over-estimated by 1.4 °C at Marambio Island and by 0.8 °C at Abernethy Flats and ~~by~~ 0.6 °C at the Johann Gregor Mendel borehole sites. MAGT was over-estimated by only 0.2 °C at the Hope Bay mainland site which suggests that there was a continuous gradient of MAGT over-estimation from the Eastern Antarctic Peninsula to MAGT under-estimation on the Western Antarctic Peninsula.

4.2 Permafrost controls

The modelled permafrost temperatures reflect the climatic characteristics of the Antarctic with major controls of latitude, elevation and continentality (Vieira et al., 2010). The effects of the ocean and continentality are well reflected in altitudinal MAGT profiles in Figs 16 and 17. Regions with areas close to the open sea generally show faster MAGT decrease with elevation, which was observed especially in the Vestfold Hills, the Transantarctic Mountains east of ~~the~~ 90° meridian, and in Marie Byrd Land, where the MAGT dropped significantly with the first elevation increase of 100 or 200 m. The same phenomenon was observed in the North Antarctic Peninsula, on the South Shetland Islands, ~~the~~ Palmer Archipelago, and on the West Antarctic Peninsula mainland, where there is less sea ice ~~presence in comparison to~~ than on James Ross Island and the West Antarctic Peninsula mainland where ~~this~~ MAGT decrease was not observed. The continental mountainous regions of the Ellsworth Mountains, and the Transantarctic Mountains west of the 90° meridian, have, ~~on the other hand,~~ no open sea in the vicinity and had a significantly slower MAGT drop with the altitude.

The modelled MAGT lapse rate of 0.40 °C 100 m⁻¹ for the whole Antarctic is lower than the average air temperature lapse rate of 0.65 °C 100 m⁻¹ in the International Standard Atmosphere (ISO 2533:1975) but is,

however, the same as the mean air temperature lapse rate measured for ice-free sites on James Ross Island from 2013–2016 (Ambrozova et al., 2019). Small increases ~~of~~in MAGTs with elevation were observed in many regions. This might be attributed to the nature of the analysis rather than a presence of temperature inversions. The rock outcrops on the scale of the regions are often present at different elevations far from each other, which results in occurrence of higher MAGTs at higher elevations. Additionally, some elevation bins have only a few rock outcrop pixels, which makes the averaged MAGT less representative for the whole region.

The lowest MAGT ensemble mean of -33.5 °C was modelled in the Transantarctic Mountains at the Queen Elizabeth Range, where the highest peak reaches 4350 m. The MAGT there could fall below -36 °C according to the coldest ensemble member. This is the lowest MAGT modelled on Earth according to the modelling in the other parts of the globe (Obu et al., ~~2019~~2019a, Obu et al., 2019b). On the highest Antarctic peak, Mount Vinson in the Ellsworth Mountains reaching 4892 m, a MAGT of only -26.1 °C was modelled. The Queen Elizabeth Range lies approximately 5° further south than Mount Vinson, illustrating the effect of latitude on permafrost temperatures.

~~The~~ winter air temperature inversions that occur in the McMurdo Dry Valleys result in air temperatures that are approx. about 10 °C lower in the valleys than in the surroundings, but inversions are occasionally disrupted by ~~katabatic winds from the polar ice sheet (Nylen et al., 2004)~~winter storms. The winter inversions reflect in MAGTs being approx. 3 °C colder on the floor than in surroundings in Victoria Valley, where the inversions are particularly intense in comparison to other valleys. No MAGT inversions were modelled in the Wright Valley, which lies only 50 m a.s.l (though winter temperature inversions do occur there), or in the Taylor Valley, which is opened to the coast and can drain cold air.

4.3 Model performance and limitations

~~As~~ the LST data are primarily derived from satellite data, their availability and accuracy depend on cloud cover. On one hand the frequent cloud cover might be a reason for general under-estimation of modelled MAGT at Antarctic Peninsula. ~~On the other hand~~However, the clear sky conditions in the McMurdo Dry Valleys might explain the relatively successful modelling results in this area.

The absence of vegetation in the Antarctic results in high snow redistribution by wind and highly spatially variable snow cover, which influences ground temperatures in many parts of the Antarctic (Guglielmin et al., 2014; Ramos et al., 2017; Ferreira et al. 2017). Neither snow redistribution nor sublimation are simulated by our snowfall model and the average snow depths could not be estimated ~~and so~~ ne-factors could not be derived as for the Antarctic, in the same manner as was done for the Northern Hemisphere by Obu et al. (~~2019~~2019a). Although an ensemble of 200 model runs with varying annual snowfall is used, the mean of the ensemble runs does not always represent the borehole site microclimate and ground properties. In the case of wind-exposed nunataks where the snow presence is over-estimated on larger areas, such as Flarjuven Bluff and Vesleskarvet, the MAGTs ~~can be were~~ over-estimated by up to 4 °C, but the modelled ensemble minimum still ~~approaches~~approached the measured MAGT.

Several permafrost and active-layer studies in the Antarctic have noted occurrence of n_f -factors above 1 (Lacelle et al., 2016; Kotzé and Meiklejohn, 2017), which indicates that average air temperatures are higher than ground surface temperatures. The likely explanation could be a presence of snow during the warmer part of the year, which is insulating ground from heat, unlike from cold in the winter. However Kotzé and Meiklejohn (2017) mention also a presence of blocky deposits at the Vesleskarvet site, which could result in ground cooling due to cold air advection. The concept of n_f -factors was introduced for the Northern Hemisphere to account for snowcoverthe effect of snow-cover during freezing conditions (Smith and Riseborough, 1996), which challenges the derivation of n_f -factors for TTOP modelling on the Antarctic sites with highly temporarily variable snow cover.

Ground properties such as water or organic matter contents could not be taken into account by r_k -factors due to the absence of datasets on a pan-Antarctic scale. However, the r_k -factors are multiplied only with TDDs in the TTOP model. The TDDs are low in comparison to FDDs in the Antarctic, which results in limited influence of the r_k -factors on the results. There were no TDDs present in the Antarctic interior according to the input data. TDDs in coastal areas usually contributed less than 1 % to the whole sum of FDDs and TDDs and this contribution increased up to 15 % at the lowland sites on the South Shetland Islands. However, ground stratigraphies are crucial for transient permafrost models in the Antarctic.

Elevation is one of the major permafrost controlling factors in the Antarctic (Vieira et al., 2010). In steep terrain, the model input datasets are less likely to be representative for the micro-locations ~~present~~ within the modelled pixel or the borehole site as, for example, shown on the ~~boreholes~~borehole sites on the walls of the Wright Valley. A number of the Antarctic boreholes are situated in mountainous environments, which might explain some of the discrepancies between measured and modelled MAGT. Elevation uncertainties in DEM are inherited by the model and reflected in the estimated average annual snowfall and downscaled ERA reanalysis temperatures. The elevations of some peaks might also not be well represented at the spatial resolution of 1 km, therefore the modelled MAGT might appear warmer than MAGT found on the top a peak.

5 Conclusions

Near-surface permafrost temperatures in the Antarctic were most commonly modelled as between -23 and -18 °C for mountainous areas rising above the Antarctic Ice Sheet. The Earth's lowest permafrost temperature of - ~~33~~36 °C was modelled at Mount Markham in the Queen Elizabeth Range in the Transantarctic Mountains. Coastal regions were usually characterised with ground temperatures of between -14 and -8 °C, approaching 0 °C in the coastal areas of the Antarctic Peninsula and rising above 0°C in the Antarctic Islands. The regional variations in permafrost temperatures can be explained by (1) continentality, which influences permafrost temperatures especially, at elevations of up to 200 m; (2) elevation; and (3) latitude, which explains differences in permafrost temperatures at similar elevations. Snow cover, and snow redistribution have strong influence on local permafrost temperature variations in the Antarctic.

Comparison of modelled temperatures to 40 permafrost boreholes and soil climate stations yielded root mean square error of 1.9 °C but the accuracy varied significantly amongbetween borehole sites. The difference was smaller than 1 °C for more than 50 % of the sites, but can exceed 4 °C. The greatest differences between the modelled and measured permafrost temperatures occurred where snow conditions were not successfully represented in the model. These sites are generally exposed to a strong wind-driven redistribution of snow as for example at nunataks in Queen Maud Land, on the Hobs Coast, and in Marie Byrd Land. Considerable differences between modelled and measured MAGTs also occurred at sites with microclimate and ground properties that are not representative for the respective modelled 1 km² pixel. Permafrost temperatures on the walls of Wright Valley and in Granite Harbour were under-estimated by up to 4 °C, which can be explained by warm microclimates of the borehole sites compared to surroundings. The model performed well in areas with frequent cloud-free conditions such as the McMurdo Dry Valleys, where even winter air temperature inversions are reflected in the modelled permafrost temperatures. Frequent cloudy conditions in the north-western Antarctic Peninsula can to some extent explain the systematic under-estimation of modelled permafrost temperatures in this area.

This study is the first continent-wide modelling of permafrost temperatures for the Antarctic. It reports near-surface permafrost temperatures for remote regions without observations, which is highly valuable for research fields, such as climate change, terrestrial ecology, microbiology or astrobiology. Our study suggests that extended networks of currently sparse borehole temperature measurements and spatially distributed information on snow cover and ground properties are crucial for improving future permafrost modelling results in the Antarctic.

Data availability: The data are available for download at: <https://doi.pangaea.de/10.1594/PANGAEA.902576>

Appendix A: List of borehole properties, measurements and modelled results

Borehole name	Latitude	Longitude	Sensor depth (cm)	Elevation (m)	Measured MAGT (°C)	MAGT calculation period	Modelled mean MAGT (°C)
Johann Gregor Mendel	-63.80000	-57.86670	75	10	-5.60	2011-2017	-4.98
Abernethy Flats	-63.88140	-57.94830	75	n/a	-6.15	2006-2016	-5.38
Bunger Hills	-66.27530	100.76000	500	7	-8.90	2008-2014	-9.09
Schirmacher Hills	-70.77177	11.73673	100	80	-8.50	2009-2016	-8.19
Larsemann Hills	-69.38669	76.37538	500	96	-7.80	2013-2015	-7.83
Larsemann	-69.40421	76.34465	300	96	-8.60	2008, 2010-2015	-7.90
Landing nunatak	-69.74781	73.70503	100	96	-11.00	2011-2012	-10.08
King George island	-62.19667	-58.96556	500	20	-0.70	2008-2009, 2014	-2.21
Hobs coast	-74.76333	-136.79639	50	76	-10.30	2008-2013	-6.86
Molodejnaya	-67.66556	45.84194	50	45	-9.40	2008, 2011-2013, 2015-2016	-7.81
Reina Sofia	-62.67028	-60.38222	n/a	275	-1.78	n/a	-3.05
Cierva Cove	-64.16195	-60.95093	1500	182	-0.95	n/a	-3.67
Amsler	-64.77619	-64.06057	900	67	-0.36	2016-2017	-1.48
Crater Lake	-62.98333	-60.66667	n/a	85	-0.83	n/a	-2.96
Byers Peninsula	-62.62981	-61.06013	n/a	92	-0.43	n/a	-2.33
Limnopolar Lake	-62.64959	-61.10405	130	90	-0.60	2009-2012	-2.34
Rothera Point	-67.57070	-68.11879	n/a	31	-3.10	2009-2011	-2.78
Marambio Island	-64.23333	-56.61667	n/a	200	-6.60	2009-2012	-5.24
Signy Island	-60.71655	-45.59978	n/a	90	-2.10	2006-2009	-2.11
Ohridski 2 Papagal	-62.64811	-60.36375	400	147	-1.04	2008-2018	-1.90
Irizar 2	-62.98263	-60.71562	80	130	-1.58	2009-2017	-2.49
Troll Station	-72.01139	2.53306	3	1275	-17.40	2007-2015	-17.09
Flarjuven Bluff	-72.01167	-3.38833	3	1220	-17.50	2008-2015	-13.06
Vesleskarvet	-71.68998	-2.84758	3	805	-16.10	2009-2014	-11.91
Boulder Clay	-74.74583	164.02139	n/a	205	-16.90	1996-2009	-14.63
Oasi New	-74.70000	164.10000	n/a	80	-13.50	2005-2009	-13.32
Bull Pass	-77.51847	161.86269	60	141	-19.44	2000-2017	-20.93
WV south wall (Bull Pass East)	-77.50219	162.06475	50	832	-16.44	2013-2017	-20.04
WV north wall (Don Juan Pond)	-77.57388	161.23877	50	734	-16.76	2011-2017	-20.83
Granite Harbour	-77.00655	162.52561	66	6	-14.31	2003-2017	-18.53
Marble Point	-77.41955	163.68247	120	47	-18.15	2000-2017	-15.99
Minna Bluff	-78.52500	166.78240	43	32	-16.44	2007-2016	-16.52
Mt. Fleming	-77.54519	160.29027	22	1697	-23.81	2002-2017	-23.58
Scott Base	-77.84831	166.76058	40	44	-17.42	2000-2017	-16.64
Victoria Valley	-77.33178	161.60069	30	410	-22.87	2000-2017	-22.97
Wright Valley Floor	-77.51808	161.85117	75	n/a	-19.13	2000-2017	-20.93
Marble Point Borehole	-77.40732	163.72913	200	85	-16.90	2009-2015	-15.96
Baker Rocks	-74.20750	164.83361	3	11	-15.60	2006-2015	-16.52
Mt. Dolence	-79.82181	-83.19714	30	886	-18.30	2012-2013	-20.21
Hope Bay	-63.40635	-56.99656	80	n/a	-4.10	2010	-3.83

Borehole name	Latitude	Longitude	Sensor depth (cm)	Elevation (m)	Measured		Modelled mean MAGT
					MAGT	MAGT calculation period	
Johann Gregor Mendel	-63.80000	-57.86670	75	10	-5.60	2011-2017	-4.98
Abernethy Flats	-63.88140	-57.94830	75	n/a	-6.15	2006-2016	-5.38
Bunger Hills	-66.27530	100.76000	500	7	-8.90	2008-2014	-9.09
Schirmacher Hills	-70.77177	11.73673	100	80	-8.50	2009-2016	-8.19
Larsemann Hills	-69.38669	76.37538	500	96	-7.80	2013-2015	-7.83
Larsemann	-69.40421	76.34465	300	96	-8.60	2008, 2010-2015	-7.90
Landing nunatak	-69.74781	73.70503	100	96	-11.00	2011-2012	-10.08
King George island	-62.19667	-58.96556	500	20	-0.70	2008-2009, 2014	-2.21
Russkaya	-74.76333	-136.79639	50	76	-10.30	2008-2013	-6.86
Molodejnaya	-67.66556	45.84194	50	45	-9.40	2008, 2011-2013, 2015-2016	-7.81
Reina Sofia	-62.67028	-60.38222	n/a	275	-1.78	n/a	-3.05
Cierva Cove	-64.16195	-60.95093	1500	182	-0.95	n/a	-3.67
Amsler	-64.77619	-64.06057	900	67	-0.36	2016-2017	-1.48
Crater Lake	-62.98333	-60.66667	n/a	85	-0.83	n/a	-2.96
Byers Peninsula	-62.62981	-61.06013	n/a	92	-0.43	n/a	-2.33
Limnopolar Lake	-62.64959	-61.10405	130	90	-0.60	2009-2012	-2.34
Rothera Point	-67.57070	-68.11879	n/a	31	-3.10	2009-2011	-2.78
Marambio Island	-64.23333	-56.61667	n/a	200	-6.60	2009-2012	-5.24
Signy Island	-60.71655	-45.59978	n/a	90	-2.10	2006-2009	-2.11
Ohridski 2 Papagal	-62.64811	-60.36375	400	147	-1.04	2008-2018	-1.90
Irizar 2	-62.98263	-60.71562	80	130	-1.58	2009-2017	-2.49
Troll Station	-72.01139	2.53306	3	1275	-17.40	2007-2015	-17.09
Flarjuven Bluff	-72.01167	-3.38833	3	1220	-17.50	2008-2015	-13.06
Vesleskarvet	-71.68998	-2.84758	3	805	-16.10	2009-2014	-11.91
Boulder Clay	-74.74583	164.02139	n/a	205	-16.90	1996-2009	-14.63
Oasi New	-74.70000	164.10000	n/a	80	-13.50	2005-2009	-13.32
Bull Pass	-77.51847	161.86269	60	141	-19.44	2000-2017	-20.93
WV south wall (Bull Pass East)	-77.50219	162.06475	50	832	-16.44	2013-2017	-20.04
WV north wall (Don Juan Pond)	-77.57388	161.23877	50	734	-16.76	2011-2017	-20.83
Granite Harbour	-77.00655	162.52561	66	6	-14.31	2003-2017	-18.53
Marble Point	-77.41955	163.68247	120	47	-18.15	2000-2017	-15.99
Minna Bluff	-78.52500	166.78240	43	32	-16.44	2007-2016	-16.52
Mt. Fleming	-77.54519	160.29027	22	1697	-23.81	2002-2017	-23.58
Scott Base	-77.84831	166.76058	40	44	-17.42	2000-2017	-16.64
Victoria Valley	-77.33178	161.60069	30	410	-22.87	2000-2017	-22.97
Wright Valley Floor	-77.51808	161.85117	75	n/a	-19.13	2000-2017	-20.93
Marble Point Borehole	-77.40732	163.72913	200	85	-16.90	2009-2015	-15.96
Baker Rocks	-74.20750	164.83361	3	11	-15.60	2006-2015	-16.52
Mt. Dolence	-79.82181	-83.19714	30	886	-18.30	2012-2013	-20.21
Hope Bay	-63.40635	-56.99656	80	n/a	-4.10	2010	-3.83

Appendix A: (Continuation)

Borehole name	Difference between Modelled Modelled			Modelled SD (°C)	Source	Soil Region
	modelled and measured MAGT (°C)	max MAGT	min MAGT			
Johann Gregor Mendel	0.62	-2.83	-6.43	0.89	Hrbáček et al., 2017a	Antarctic Peninsula
Abernethy Flats	0.77	-2.89	-6.89	1.08	Hrbáček et al., 2017b	Antarctic Peninsula
Bunger Hills	-0.19	-4.41	-11.50	1.41	Andrey Abramov	Wilkes Land
Schirmacher Hills	0.31	-3.91	-9.95	1.08	Andrey Abramov	Queen Maud Land
Larsemann Hills	-0.03	-3.53	-9.82	1.23	Andrey Abramov	Vestfold Hills
Larsemann	0.70	-3.64	-9.76	1.17	Andrey Abramov	Vestfold Hills
Landing nunatak	0.93	-6.10	-12.39	1.33	Andrey Abramov	Vestfold Hills
King George island	-1.51	-0.93	-2.75	0.47	Andrey Abramov	Antarctic Peninsula
Hobs coast	3.44	-4.06	-10.14	1.66	Andrey Abramov	Marie Byrd Land
Molodejnaya	1.59	-4.06	-10.19	1.66	Andrey Abramov	Enderby Land
Reina Sofia	-1.27	-1.54	-3.97	0.67	Miguel Ramos	Antarctic Peninsula
Cierva Cove	-2.72	-1.95	-5.51	0.86	Gonçalo Vieira	Antarctic Peninsula
Amsler	-1.12	-0.65	-2.42	0.49	Gonçalo Vieira	Antarctic Peninsula
Crater Lake	-2.13	-1.51	-4.01	0.65	Gonçalo Vieira	Antarctic Peninsula
Byers Peninsula	-1.90	-1.10	-2.95	0.50	Oliva et al. (2017)	Antarctic Peninsula
Limnopolar Lake	-1.74	-1.04	-2.90	0.47	de Pablo et al. (2014)	Antarctic Peninsula
Rothera Point	0.32	-1.36	-3.95	0.74	Guglielmin et al. (2014)	Antarctic Peninsula
Marambio Island	1.36	-3.01	-6.58	0.83	Jorge Strelin	Antarctic Peninsula
Signy Island	-0.01	-0.97	-2.86	0.45	Guglielmin et al. (2012)	Antarctic Islands
Ohridski 2 Papagal	-0.87	-0.93	-2.80	0.43	Gonçalo Vieira	Antarctic Peninsula
Irizar 2	-0.91	-1.21	-3.33	0.60	Gonçalo Vieira	Antarctic Peninsula
Troll Station	0.31	-9.41	-19.56	1.19	Hrbáček et al. (2018)	Queen Maud Land
Flarjuven Bluff	4.45	-6.46	-16.84	2.68	Hrbáček et al. (2018)	Queen Maud Land
Vesleskarvet	4.19	-6.01	-15.09	2.57	Hrbáček et al. (2018)	Queen Maud Land
Boulder Clay	2.27	-8.83	-16.78	1.22	Vieira et al. (2010)	Transantarctic Mountains
Oasi New	0.18	-8.24	-15.08	0.84	Vieira et al. (2010)	Transantarctic Mountains
Bull Pass	-1.49	-17.24	-22.65	0.95	USDA (Seybold et al., 2009)	Transantarctic Mountains
WV south wall (Bull Pass East)	-3.60	-17.35	-21.64	0.90	Megan Balks	Transantarctic Mountains
WV north wall (Don Juan Pond)	-4.07	-18.33	-22.50	0.82	Megan Balks	Transantarctic Mountains
Granite Harbour	-4.22	-15.52	-20.15	0.84	USDA (Seybold et al., 2009)	Transantarctic Mountains
Marble Point	2.16	-13.67	-17.83	0.65	Megan Balks	Transantarctic Mountains
Minna Bluff	-0.07	-10.74	-19.03	1.35	Megan Balks	Transantarctic Mountains
Mt. Fleming	0.23	-19.36	-25.66	1.01	Megan Balks	Transantarctic Mountains
Scott Base	0.78	-10.72	-18.84	1.08	Megan Balks	Transantarctic Mountains
Victoria Valley	-0.10	-21.26	-24.59	0.90	Megan Balks	Transantarctic Mountains
Wright Valley Floor	-1.79	-17.24	-22.65	0.95	Megan Balks	Transantarctic Mountains
Marble Point Borehole	0.95	-11.46	-17.72	0.83	Guglielmin et al. (2011)	Transantarctic Mountains
Baker Rocks	-0.92	-7.11	-19.39	1.59	Hrbáček et al. (2018)	Transantarctic Mountains
Mt. Dolence	-1.91	-13.48	-22.37	1.13	Schaefer et al. (2017b)	Ellsworth Mountains
Hope Bay	0.27	-1.82	-4.97	0.66	Schaefer et al. (2017a)	Antarctic Peninsula

Borehole name	Difference between		Modelled	Modelled	Modelled SD	Source	Soil Region
	modelled and measured MAGT	max MAGT	min MAGT				
Johann Gregor Mendel	0.62	-2.83	-6.43	0.89	Hrbáček et al., 2017a	Antarctic Peninsula	
Abernethy Flats	0.77	-2.89	-6.89	1.08	Hrbáček et al., 2017b	Antarctic Peninsula	
Bunger Hills	-0.19	-4.41	-11.50	1.41	Andrey Abramov	Wilkes Land	
Schirmacher Hills	0.31	-3.91	-9.95	1.08	Andrey Abramov	Queen Maud Land	
Larsemann Hills	-0.03	-3.53	-9.82	1.23	Andrey Abramov	Vestfold Hills	
Larsemann	0.70	-3.64	-9.76	1.17	Andrey Abramov	Vestfold Hills	
Landing nunatak	0.93	-6.10	-12.39	1.33	Andrey Abramov	Vestfold Hills	
King George island	-1.51	-0.93	-2.75	0.47	Andrey Abramov	Antarctic Peninsula	
Russkaya	3.44	-4.06	-10.14	1.66	Andrey Abramov	Marie Byrd Land	
Molodejnaya	1.59	-4.06	-10.19	1.66	Andrey Abramov	Enderby Land	
Reina Sofia	-1.27	-1.54	-3.97	0.67	Miguel Ramos	Antarctic Peninsula	
Cierva Cove	-2.72	-1.95	-5.51	0.86	Gonçalo Vieira	Antarctic Peninsula	
Amsler	-1.12	-0.65	-2.42	0.49	Gonçalo Vieira	Antarctic Peninsula	
Crater Lake	-2.13	-1.51	-4.01	0.65	Gonçalo Vieira	Antarctic Peninsula	
Byers Peninsula	-1.90	-1.10	-2.95	0.50	Oliva et al. (2017)	Antarctic Peninsula	
Limnopolar Lake	-1.74	-1.04	-2.90	0.47	de Pablo et al. (2014)	Antarctic Peninsula	
Rothera Point	0.32	-1.36	-3.95	0.74	Guglielmin et al. (2014)	Antarctic Peninsula	
Marambio Island	1.36	-3.01	-6.58	0.83	Jorge Strelin	Antarctic Peninsula	
Signy Island	-0.01	-0.97	-2.86	0.45	Guglielmin et al. (2012b)	Antarctic Islands	
Ohridski 2 Papagal	-0.87	-0.93	-2.80	0.43	Gonçalo Vieira	Antarctic Peninsula	
Irizar 2	-0.91	-1.21	-3.33	0.60	Gonçalo Vieira	Antarctic Peninsula	
Troll Station	0.31	-9.41	-19.56	1.19	Hrbáček et al. (2018)	Queen Maud Land	
Flarjuven Bluff	4.45	-6.46	-16.84	2.68	Hrbáček et al. (2018)	Queen Maud Land	
Vesleskarvet	4.19	-6.01	-15.09	2.57	Hrbáček et al. (2018)	Queen Maud Land	
Boulder Clay	2.27	-8.83	-16.78	1.22	Vieira et al. (2010)	Transantarctic Mountains	
Oasi New	0.18	-8.24	-15.08	0.84	Vieira et al. (2010)	Transantarctic Mountains	
Bull Pass	-1.49	-17.24	-22.65	0.95	USDA (Seybold et al., 2009)	Transantarctic Mountains	
WV south wall (Bull Pass East)	-3.60	-17.35	-21.64	0.90	Megan Balks	Transantarctic Mountains	
WV north wall (Don Juan Pond)	-4.07	-18.33	-22.50	0.82	Megan Balks	Transantarctic Mountains	
Granite Harbour	-4.22	-15.52	-20.15	0.84	USDA (Seybold et al., 2009)	Transantarctic Mountains	
Marble Point	2.16	-13.67	-17.83	0.65	Megan Balks	Transantarctic Mountains	
Minna Bluff	-0.07	-10.74	-19.03	1.35	Megan Balks	Transantarctic Mountains	
Mt. Fleming	0.23	-19.36	-25.66	1.01	Megan Balks	Transantarctic Mountains	
Scott Base	0.78	-10.72	-18.84	1.08	Megan Balks	Transantarctic Mountains	
Victoria Valley	-0.10	-21.26	-24.59	0.90	Megan Balks	Transantarctic Mountains	
Wright Valley Floor	-1.79	-17.24	-22.65	0.95	Megan Balks	Transantarctic Mountains	
Marble Point Borehole	0.95	-11.46	-17.72	0.83	Guglielmin et al. (2011)	Transantarctic Mountains	
Baker Rocks	-0.92	-7.11	-19.39	1.59	Hrbáček et al. (2018)	Transantarctic Mountains	
Mt. Dolence	-1.91	-13.48	-22.37	1.13	Schaefer et al. (2017b)	Ellsworth Mountains	
Hope Bay	0.27	-1.82	-4.97	0.66	Schaefer et al. (2017a)	Antarctic Peninsula	

Author contribution: JO, SW, GV, AB and AK designed conceptual framework for the study and the model was developed and ran by SW and JO. Ground validation data was contributed by GV, AA, MB, FH and MR, who also provided interpretation of results on regional scale. JO wrote the paper based from input and feedback from all co-authors.

Competing interests: The authors declare that they have no conflict of interest.

Acknowledgements: This work was funded by the European Space Agency Data User Element GlobPermafrost project in cooperation with ZAMG (grant number 4000116196/15/I-NB) and the Research Council of Norway SatPerm project (grant number 239918). Data storage resources were provided by Norwegian National Infrastructure for Research Data (project NS9079K). The work of FH was supported by the Ministry of Education Youth and Sports of Czech Republic large infrastructure project LM2015078. Temperature data for Russian stations were obtained with the support ~~from~~ from the Russian Antarctic Expedition and Government program AAAA-A18-118013190181-6. The PERMANTAR observatories in Western Antarctic Peninsula have been funded mainly by the Portuguese Foundation for Science and Technology and the Portuguese Polar Program. The Terra and AQUA MODIS LST datasets were acquired from the Level-1 and Atmosphere Archive & Distribution System (LAADS) Distributed Active Archive Center (DAAC), located in the Goddard Space Flight Center in Greenbelt, Maryland (<https://ladsweb.nascom.nasa.gov/>). Over the years many people have contributed to installation and maintenance of the McMurdo Dry Valley Soil Climate stations, but particular thanks are due to Cathy Seybold, Ron Paetzold and Don Huffman from USDA, Jackie Aislabie and Fraser Morgan, Landcare Research, N.Z., and Chris Morcom, Dean Sandwell, and Annette Carshalton, University of Waikato, NZ. Antarctica New Zealand provided logistic support for annual station access. Authors thank also to Nikita Demidov, Andrey Dolgikh, Elya Zazovskaya, Nikolay Osokin, Dima Fedorov-Davidov, Andrey Ivashchenko, Alexey Lupachev and Nikita Mergelov for borehole data retrieval from the Russian Antarctic Stations.

References

- Ambrozova, K., Laska, K., Hrbacek, F., Kavan, J. and Ondruch, J.: Air temperature and lapse rate variation in the ice-free and glaciated areas of northern James Ross Island, Antarctic Peninsula, during 2013–2016, *International Journal of Climatology*, 39(2), 643–657, doi:10.1002/joc.5832, 2019.
- Beer, C.: Permafrost Sub-grid Heterogeneity of Soil Properties Key for 3-D Soil Processes and Future Climate Projections, *Front. Earth Sci.*, 4, doi:10.3389/feart.2016.00081, 2016.
- Bintanja, R. and Reijmer, C. H.: A simple parameterization for snowdrift sublimation over Antarctic snow surfaces, *Journal of Geophysical Research: Atmospheres*, 106(D23), 31739–31748, doi:10.1029/2000JD000107, 2001.
- Bockheim, J., Vieira, G., Ramos, M., López-Martínez, J., Serrano, E., Guglielmin, M., Wilhelm, K. and Nieuwendam, A.: Climate warming and permafrost dynamics in the Antarctic Peninsula region, *Global and Planetary Change*, 100, 215–223, doi:10.1016/j.gloplacha.2012.10.018, 2013.
- Bockheim, J. G., Campbell, I. B. and McLeod, M.: Permafrost distribution and active-layer depths in the McMurdo Dry Valleys, Antarctica, *Permafrost and Periglacial Processes*, 18(3), 217–227, doi:10.1002/ppp.588, 2007.

Bockheim, J. G., Campbell, I. B., Guglielmin, M. and López-Martínez, J.: Distribution of permafrost types and buried ice in icefree areas of Antarctica, in 9th International Conference on Permafrost, Proceedings. University of Alaska Press: Fairbanks, pp. 125–130., 2008.

Burton-Johnson, A., Black, M., Fretwell, P. T. and Kaluza-Gilbert, J.: An automated methodology for differentiating rock from snow, clouds and sea in Antarctica from Landsat 8 imagery: a new rock outcrop map and area estimation for the entire Antarctic continent, *The Cryosphere*, 10(4), 1665–1677; doi:<https://doi.org/10.5194/tc-10-1665-2016>, 2016.

Danielson, J. J. and Gesch, D. B.: Global multi-resolution terrain elevation data 2010 (GMTED2010), *USGS Numbered Series, U.S. Geological Survey*. [online] Available from: <http://pubs.er.usgs.gov/publication/ofr20111073> (Accessed 9 October 2018); *US Geological Survey*, 2011.

de Pablo, M. A., Ramos, M. and Molina, A.: Thermal characterization of the active layer at the Limnopolar Lake CALM-S site on Byers Peninsula (Livingston Island), *Antarctica, Solid Earth*, 5(2), 721–739, doi:<https://doi.org/10.5194/se-5-721-2014>, 2014.

de Pablo, M. A., Ramos, M. and Molina, A.: Snow cover evolution, on 2009-2014, at the Limnopolar Lake CALM-S site on Byers Peninsula, Livingston Island, Antarctica., *CATENA*, 149, 538–547, doi:10.1016/j.catena.2016.06.002, 2017.

Decker, E. R. and Bucher, G. J.: Geothermal studies in Antarctica, *Antarct. J. U. S.; (United States)*, 12:4 [online] Available from: <https://www.osti.gov/biblio/6112190> (Accessed 29 April 2019), 1977.

Dee, D. P., Uppala, S. M., Simmons, A. J., Berrisford, P., Poli, P., Kobayashi, S., Andrae, U., Balmaseda, M. A., Balsamo, G., Bauer, P., Bechtold, P., Beljaars, A. C. M., Berg, L. van de, Bidlot, J., Bormann, N., Delsol, C., Dragani, R., Fuentes, M., Geer, A. J., Haimberger, L., Healy, S. B., Hersbach, H., Hólm, E. V., Isaksen, I., Kållberg, P., Köhler, M., Matricardi, M., McNally, A. P., Monge-Sanz, B. M., Morcrette, J.-J., Park, B.-K., Peubey, C., Rosnay, P. de, Tavolato, C., Thépaut, J.-N. and Vitart, F.: The ERA-Interim reanalysis: configuration and performance of the data assimilation system, *Quarterly Journal of the Royal Meteorological Society*, 137(656), 553–597, doi:10.1002/qj.828, 2011.

Ferreira, A., Vieira, G., Ramos, M. and Nieuwendam, A.: Ground temperature and permafrost distribution in Hurd Peninsula (Livingston Island, Maritime Antarctic): An assessment using freezing indexes and TTOP modelling, *CATENA*, 149, 560–571, doi:10.1016/j.catena.2016.08.027, 2017.

Fiddes, J. and Gruber, S.: TopoSCALE v.1.0: downscaling gridded climate data in complex terrain, *Geosci. Geoscientific Model Dev., Development*, 7(1), 387–405, doi:<https://doi.org/10.5194/gmd-7-387-2014>, 2014.

Gallée, H.: Simulation of blowing snow over the antarctic ice sheet, *Annals of Glaciology*, 26, 203–206, doi:10.3189/1998AoS26-1-203-206, 1998.

Gisnås, K., Eitzel Müller, B., Farbrøt, H., Schuler, T. V. and Westermann, S.: CryoGRID 1.0: Permafrost Distribution in Norway estimated by a Spatial Numerical Model, *Permafrost and Periglacial Processes*, 24(1), 2–19, doi:10.1002/ppp.1765, 2013.

Gisnås, K., Westermann, S., Schuler, T. V., Litherland, T., Isaksen, K., Boike, J. and Eitzel Müller, B.: A statistical approach to represent small-scale variability of permafrost temperatures due to snow cover, *The Cryosphere*, 8(6), 2063–2074, doi:<https://doi.org/10.5194/tc-8-2063-2014>, 2014.

Greene, S. W., Gressitt, J. L., Koob, D., Llano, G. A., Rudolph, E. D., Singer, R., Steere, W. C. and Ugolini, F. C.: Terrestrial life of Antarctica. *Antarctic Map Folio Series*, Nat. Geogr. Soc. New York, 1967.

Guglielmin, M.: *Advances in permafrost and periglacial research in Antarctica: A review*, *Geomorphology*, 155–156, 1–6, doi:10.1016/j.geomorph.2011.12.008, 2012a.

Guglielmin, M.: Ground surface temperature (GST), active layer and permafrost monitoring in continental Antarctica, *Permafrost and Periglacial Processes*, 17(2), 133–143, doi:10.1002/ppp.553, 2006.

Guglielmin, M.: *Advances in permafrost and periglacial research in Antarctica: A review*, *Geomorphology*, 155–156, 1–6, doi:10.1016/j.geomorph.2011.12.008, 2012.

Guglielmin, M., Balks, M. R., Adlam, L. S. and Baio, F.: Permafrost thermal regime from two 30-m deep boreholes in southern Victoria Land, Antarctica, *Permafrost and Periglacial Processes*, 22(2), 129–139, doi:10.1002/ppp.715, 2011.

Guglielmin, M., Worland, M. R. and Cannone, N.: Spatial and temporal variability of ground surface temperature and active layer thickness at the margin of maritime Antarctica, Signy Island, *Geomorphology*, 155–156, 20–33, doi:10.1016/j.geomorph.2011.12.016, [20122012b](#).

Guglielmin, M., Worland, M. R., Baio, F. and Convey, P.: Permafrost and snow monitoring at Rothera Point (Adelaide Island, Maritime Antarctica): Implications for rock weathering in cryotic conditions, *Geomorphology*, 225, 47–56, doi:10.1016/j.geomorph.2014.03.051, 2014.

Hersbach, H. and Dee, D.: ERA5 reanalysis is in production, ECMWF [Newsletternewsletter](#), 147, ~~ECMWF~~, (7), [5–6](#), 2016.

Hevesi, J. A., Istok, J. D. and Flint, A. L.: Precipitation Estimation in Mountainous Terrain Using Multivariate Geostatistics. Part I: Structural Analysis, *J. Appl. Meteor.*, 31(7), 661–676, doi:10.1175/1520-0450(1992)031<0661:PEIMTU>2.0.CO;2, 1992.

Hrbáček, F., Kňázková, M., Nývlt, D., Láska, K., Mueller, C. W. and Ondruch, J.: Active layer monitoring at CALM-S site near J.G.Mendel Station, James Ross Island, eastern Antarctic Peninsula, *Science of The Total Environment*, 601–602, 987–997, doi:10.1016/j.scitotenv.2017.05.266, 2017a.

Hrbáček, F., Nývlt, D. and Láska, K.: Active layer thermal dynamics at two lithologically different sites on James Ross Island, Eastern Antarctic Peninsula, *CATENA*, 149, 592–602, doi:10.1016/j.catena.2016.06.020, 2017b.

Hrbáček, F., Láska, K. and Engel, Z.: Effect of Snow Cover on the Active-Layer Thermal Regime – A Case Study from James Ross Island, Antarctic Peninsula, *Permafrost and Periglacial Processes*, 27(3), 307–315, doi:10.1002/ppp.1871, 2016.

Hrbáček, F., Vieira, G., Oliva, M., Balks, M., Guglielmin, M., Pablo, M. Á. de, Molina, A., Ramos, M., Goyanes, G., Meiklejohn, I., Abramov, A., Demidov, N., Fedorov-Davydov, D., Lupachev, A., Rivkina, E., Láska, K., Kňázková, M., Nývlt, D., Raffi, R., Strelin, J., Sone, T., Fukui, K., Dolgikh, A., Zazovskaya, E., Mergelov, N., Osokin, N. and Miamin, V.: Active layer monitoring in Antarctica: an overview of results from 2006 to 2015, *Polar Geography*, 0(0), 1–15, doi:10.1080/1088937X.2017.1420105, 2018.

Humlum, O., Instanes, A. and Sollid, J. L.: Permafrost in Svalbard: a review of research history, climatic background and engineering challenges, *Polar Research*, 22(2), 191–215, doi:10.3402/polar.v22i2.64551111/j.1751-8369.2003.tb00107.x, 2003.

Kotzé, C. and Meiklejohn, I.: Temporal variability of ground thermal regimes on the northern buttress of the Vesleskarvet nunatak, western Dronning Maud Land, Antarctica, *Antarctic Science*, 29(1), 73–81, doi:10.1017/S095410201600047X, 2017.

Lacelle, D., Lapalme, C., Davila, A. F., Pollard, W., Marinova, M., Heldmann, J. and McKay, C. P.: Solar Radiation and Air and Ground Temperature Relations in the Cold and Hyper-Arid Quartermain Mountains, McMurdo Dry Valleys of Antarctica, *Permafrost and Periglacial Processes*, 27(2), 163–176, doi:10.1002/ppp.1859, 2016.

[Levy, J.: How big are the McMurdo Dry Valleys? Estimating ice-free area using Landsat image data, *Antarctic Science*, 25\(1\), 119–120, doi:10.1017/S0954102012000727, 2013.](#)

Liston, G. E.: Representing Subgrid Snow Cover Heterogeneities in Regional and Global Models, *J. Climate*, 17(6), 1381–1397, doi:10.1175/1520-0442(2004)017<1381:RSSCHI>2.0.CO;2, 2004.

[Nylen, T. H., Fountain, A. G. and Doran, P. T.: Climatology of katabatic winds in the McMurdo dry valleys, southern Victoria Land, Antarctica, *Journal of Geophysical Research: Atmospheres*, 109\(D3\), doi:10.1029/2003JD003937, 2004.](#)

[Obu, J., Westermann, S., Käab, A. and Bartsch, A.: Ground Temperature Map, 2000–2016, Andes, New Zealand and East African Plateau Permafrost, University of Oslo, doi:https://doi.org/10.1594/PANGAEA.905512, 2019b.](#)

Obu, J., Westermann, S., Bartsch, A., Berdnikov, N., Christiansen, H. H., Dashtseren, A., Delaloye, R., Elberling, B., Etzelmüller, B., Kholodov, A., Khomutov, A., Käab, A., Leibman, M. O., Lewkowicz, A. G., Panda, S. K., Romanovsky, V., Way, R. G., Westergaard-Nielsen, A., Wu, T., Yamkhin, J. and Zou, D.: Northern Hemisphere permafrost map based on TTOP modelling for 2000–2016 at 1 km² scale, *Earth-Science Reviews*, 193, 299–316, doi:10.1016/j.earscirev.2019.04.023, [20192019a](#).

Oliva, M., Hrbáček, F., Ruiz-Fernández, J., de Pablo, M. Á., Vieira, G., Ramos, M. and Antoniadou, D.: Active layer dynamics in three topographically distinct lake catchments in Byers Peninsula (Livingston Island, Antarctica), *CATENA*, 149, 548–559, doi:10.1016/j.catena.2016.07.011, 2017.

Østby, T. I., Schuler, T. V. and Westermann, S.: Severe cloud contamination of MODIS Land Surface Temperatures over an Arctic ice cap, Svalbard, *Remote Sensing of Environment*, 142, 95–102, doi:10.1016/j.rse.2013.11.005, 2014.

~~de Pablo, M. A., Ramos, M. and Molina, A.: Thermal characterization of the active layer at the Linnopolar Lake CALM S site on Byers Peninsula (Livingston Island), Antarctica, *Solid Earth*, 5(2), 721–739, doi:https://doi.org/10.5194/se-5-721-2014, 2014.~~

~~de Pablo, M. A., Ramos, M. and Molina, A.: Snow cover evolution, on 2009–2014, at the Linnopolar Lake CALM S site on Byers Peninsula, Livingston Island, Antarctica., *CATENA*, 149, 538–547, doi:10.1016/j.catena.2016.06.002, 2017.~~

Raffi, R. and Stenni, B.: Isotopic composition and thermal regime of ice wedges in northern Victoria Land, East Antarctica, *Permafrost and Periglacial Processes*, 22(1), 65–83, doi:10.1002/ppp.701, 2011.

Ramos, M., Vieira, G., de Pablo, M. A., Molina, A., Abramov, A. and Goyanes, G.: Recent shallowing of the thaw depth at Crater Lake, Deception Island, Antarctica (2006–2014), *CATENA*, 149, 519–528, doi:10.1016/j.catena.2016.07.019, 2017.

Rocha, M. J., Dutra, E., Tomé, R., Vieira, G., Miranda, P., Frago, M. and Ramos, M.: ERA-Interim forced H-TESSEL scheme for modeling ground temperatures for Livingston Island (South Shetlands, Antarctic Peninsula), in *Proceedings of II Iberian Conference of the International Permafrost Association: Periglacial, Environments, Permafrost and Climate Variability: Colección Obras colectivas*, Universidad de Alcalá., 2010.

Romanovsky, V. E. and Osterkamp, T. E.: Interannual variations of the thermal regime of the active layer and near-surface permafrost in northern Alaska, *Permafrost and Periglacial Processes*, 6(4), 313–335, doi:10.1002/ppp.3430060404, 1995.

[Roth, G., Matsuoka, K., Skoglund, A., Melvær, Y. and Tronstad, S.: Quantarctica: A Unique, Open, Standalone GIS Package for Antarctic Research and Education, in EGU General Assembly Conference Abstracts, vol. 19, p. 1973., 2017.](#)

Schaefer, C. E. G. R., Michel, R. F. M., Delpupo, C., Senra, E. O., Bremer, U. F. and Bockheim, J. G.: Active layer thermal monitoring of a Dry Valley of the Ellsworth Mountains, Continental Antarctica, *CATENA*, 149, 603–615, doi:10.1016/j.catena.2016.07.020, 2017b.

Schaefer, C. E. G. R., Pereira, T. T. C., Almeida, I. C. C., Michel, R. F. M., Corrêa, G. R., Figueiredo, L. P. S. and Ker, J. C.: Penguin activity modify the thermal regime of active layer in Antarctica: A case study from Hope Bay, *CATENA*, 149, 582–591, doi:10.1016/j.catena.2016.07.021, 2017a.

Shiklomanov, N. I.: From Exploration to Systematic Investigation: Development of Geocryology in 19th- and Early—20th-Century Russia, *Physical Geography*, 26(4), 249–263, doi:10.2747/0272-3646.26.4.249, 2005.

Smith, M. W. and Riseborough, D. W.: Permafrost monitoring and detection of climate change, *Permafrost Periglac. Process., and Periglacial Processes*, 7(4), 301–309, doi:10.1002/(SICI)1099-1530(199610)7:4<301::AID-PPP231>3.0.CO;2-R, 1996.

Smith, M. W. and Riseborough, D. W.: Climate and the limits of permafrost: a zonal analysis, *Permafrost Periglac. Process., and Periglacial Processes*, 13(1), 1–15, doi:10.1002/ppp.410, 2002.

~~Soliman, A., Duguay, C., Saunders, W., Hachem, S., Soliman, A., Duguay, C., Saunders, W. and Hachem, S.: Pan-Arctic Land Surface Temperature from MODIS and AATSR: Product Development and Intercomparison, *Remote Sensing*, 4(12), 3833–3856, doi:10.3390/rs4123833, 2012.~~

Vieira, G., Bockheim, J., Guglielmin, M., Balks, M., Abramov, A. A., Boelhouwers, J., Cannone, N., Ganzert, L., Gilichinsky, D. A., Goryachkin, S., López-Martínez, J., Meiklejohn, I., Raffi, R., Ramos, M., Schaefer, C., Serrano, E., Simas, F., Sletten, R. and Wagner, D.: Thermal state of permafrost and active-layer monitoring in the antarctic: Advances during the international polar year 2007–2009, *Permafrost and Periglacial Processes*, 21(2), 182–197, doi:10.1002/ppp.685, 2010.

Wan, Z.: New refinements and validation of the collection-6 MODIS land-surface temperature/emissivity product, *Remote Sensing of Environment*, 140, 36–45, doi:10.1016/j.rse.2013.08.027, 2014.

Westermann, S., Østby, T. I., Gislås, K., Schuler, T. V. and Etzelmüller, B.: A ground temperature map of the North Atlantic permafrost region based on remote sensing and reanalysis data, *The Cryosphere*, 9(3), 1303–1319, doi:https://doi.org/10.5194/tc-9-1303-2015, 2015.

Zhang, Y., Olthof, I., Fraser, R. and Wolfe, S. A.: A new approach to mapping permafrost and change incorporating uncertainties in ground conditions and climate projections, *The Cryosphere*, 8(6), 2177–2194, doi:<https://doi.org/10.5194/tc-8-2177-2014>, 2014.